AN ABSTRACT OF THE THESIS OF

Gregory Joseph Barone (Name) for the Doctor of Philosophy (Degree)

in General Science (Radiological Physics) (Major) presented on July 7, 1970 (Date)

Title: A COMPARATIVE STUDY OF THE DOSE DISTRIBUTION FOR THREE-PHASE AND SINGLE-PHASE X-RAY EQUIPMENT

Redacted for Privacy

Abstract approved: E. Dale Trout

There has been a large increase in the number of three-phase diagnostic x-ray systems installed in hospital special-procedure rooms during the last decade. The reason for this is the capability of three-phase systems of making possible the very short exposure times and increased tube loading required for some of the recently developed radiological procedures.

Analysis of the voltage waveforms indicates that x-ray beams produced by three-phase systems have a higher effective energy and a higher exposure rate than those produced by single-phase equipment operated at the same kilovoltage and tube current.

This study compares dose distributions for single- and three-phase x-ray systems operated under conditions similar to those used in medical radiography.

Depth-dose data were taken using thermoluminescent dosimeters in a tissue equivalent (Mix D) phantom at 40, 60, 80, 100, 125, and 150 kVp. Measurements were made at 1 cm intervals from the incident phantom surface to a depth of 13 cm, and at 2 cm intervals from 13 to 25 cm. The source to phantom surface distance was 30 inches.

Curves of equivalent kilovoltage, which would provide approximately the same radiographic results, were derived for single- and three-phase systems.

The data were normalized for equal exposures for various phantom thicknesses related to the energy used, and dose differentials were determined for both equal and equivalent kilovoltages.

A Comparative Study of the Dose Distribution for Three-Phase and Single-Phase X-Ray Equipment

by

Gregory Joseph Barone

A THESIS

submitted to

Oregon State University

in partial fulfillment of
the requirements for the
degree of

Doctor of Philosophy

June 1971

APPROVED:

Redacted for Privacy

Professor of Radiological Physics

in charge of major

Redacted for Privacy

Chairman of the Department of General Science

Redacted for Privacy

Dean of Graduate School

Date thesis is presented July 7, 1970

Typed by Barbara Eby for Gregory Joseph Barone

ACKNOWLEDGEMENT

The author wishes to express his appreciation to Dr. E. Dale Trout for his cooperation and assistance in carrying out this doctoral program.

Thanks are given to Mr. John P. Kelley for his many helpful suggestions and in particular for his efforts in the voltage and current calibrations of the x-ray generators used in this study.

A very special appreciation is extended to my wife, Joyce, for her many sacrifices and kind patience, understanding, and assistance throughout the years of my graduate study.

This project was made possible by the United States Public Health Service through their support of my graduate study at Oregon State University.

TABLE OF CONTENTS

LIST OF FIGURES

LIST OF TABLES

A COMPARATIVE STUDY OF THE DOSE DISTRIBUTION FOR THREE-PHASE AND SINGLE-PHASE X-RAY EQUIPMENT

I. INTRODUCTION

Single- and Three-Phase Power

Electric power is almost universally generated and distributed in three-phase for greatest efficiency and economy (33, 67, 80, 83). Three-phase distribution systems employ four wires: three lines conducting alternating current, plus a ground line, as shown in Figure 1. The current in each conductor is one-third cycle out of phase with those in the other two, as in Figure 2.

Single-phase power, which is generally provided for domestic applications and other low-power needs, may be obtained by tapping between the ground line and any one of the other three conductors of a three-phase line. The voltage and current between these conductors varies with time as a sine function, as shown in Figure 3.

Large electric motors and other high-power devices are often designed to use three-phase power because of the cost savings made possible by the use of smaller diameter wiring than is required for single-phase (78, 92).

X-Ray generating apparatus may be designed to operate either with single-phase or with three-phase power. Virtually all of the

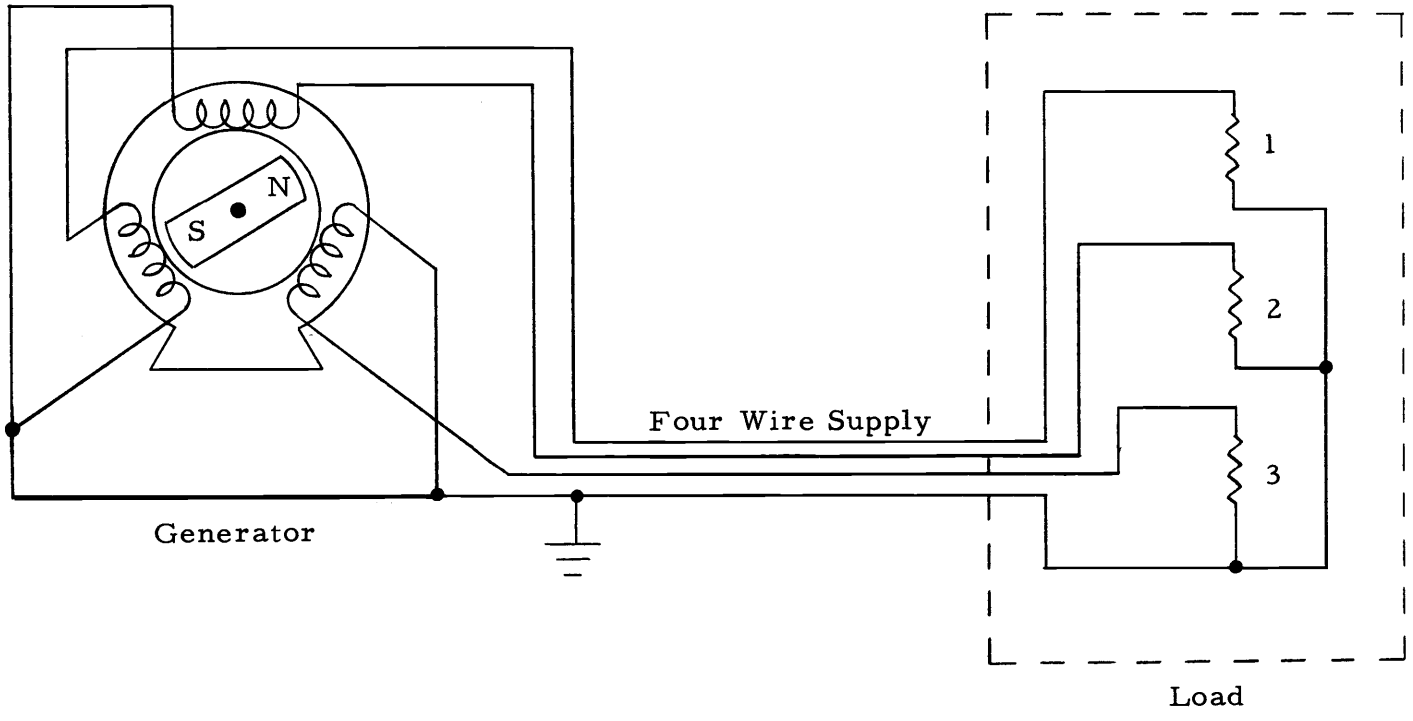

Figure 1. Three-phase generation and distribution system. Load may be three-phase or, as is shown, three single-phase loads.

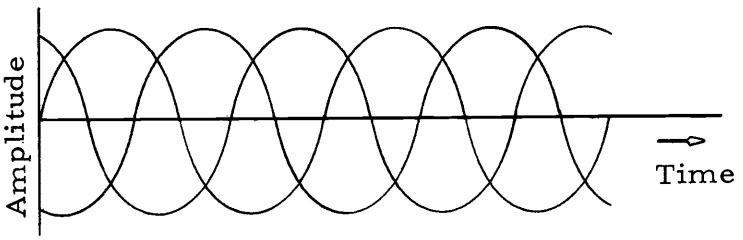

Figure 2. Waveform of three-phase alternating current distributed by power companies.

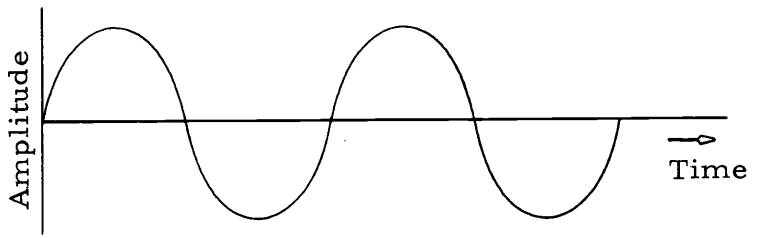

Figure 3. Waveform of single-phase alternating current.

diagnostic x-ray equipment manufactured in the United States prior to the 1960's has been single-phase (22, 102).

History of the Manufacture of Three-Phase X-Ray Generating Equipment

In 1916, K. Lasser of Siemens and Halske Co., an x-ray equipment manufacturer in Germany, showed to the Berlin Medical Society, the first three-phase x-ray generator.[1] However, it was not until the early 1920's, when Heinrich Chantraine expressed and popularized the desirability of low kilovoltage techniques as a means of obtaining better contrast in chest radiography, that three-phase equipment appeared to have any advantage over single-phase. Lower kilovoltage requires increased milliamperage to maintain the use of short exposure-time, thereby minimizing blurring due to motion. Three-phase apparatus was able to provide higher milliamperage. Probably an even greater influence in the development of three-phase x-ray generating equipment in Europe, however, was the electrical power companies' dislike of having a heavy load imposed on just one of the three phases at a time (34). Such loading induces unbalanced voltage drops in the transmission lines and transformers causing unbalanced voltages at the

[1] Dates and data concerning early manufacture of three-phase x-ray equipment have been abstracted from reference (31).

loads (2, 83)[2]. In some areas of Europe, there are restrictions placed upon the load permitted on only one phase (33, 75).

In 1924, the Koch and Sterzel Co. of Germany marketed its first three-phase x-ray transformer and in 1927, they introduced "Titanos", a 2000 mA generator. In 1928, the Siemens-Reiniger-Werke Co. of Erlangen, Germany introduced a three-phase generator providing 2000 mA at 80 kVp, and in 1929, Siemens and Halske brought out its 2000 mA "Gigantos". In 1931, Compagnie Generale de Radiologie (CGR) introduced the first French three-phase unit; the 1000 mA "Tripharix". In the later 1930's, Giampiero Clerici and Co. manufactured Italy's first three-phase generators at Milano. The DV6, which was a diagnostic unit, was rated at 600 mA and 100 kVp. The TVC6 was a six valve, two condensor unit for therapy and was rated at 10 mA and 25 kVp.

From these early beginnings, the use of three-phase x-ray generating equipment spread throughout European countries and to a lesser extent, to countries outside of Europe (64). In the United States, the only company to manufacture three-phase generators, prior to the 1960's, was the Picker X-Ray Corporation. This equipment was produced from the middle 1930's until the beginning of World War II, at

---

[2]In the United States, this problem was often circumvented by balancing several loads within a particular facility over all three phases of the distribution system (95).

which time it was discontinued.

There are several reasons for the prior lack of interest in the development of three-phase generators in this country: (1) adequate single-phase power has been readily available and unrestricted in its use, (2) three-phase generators are significantly more complicated, bulky, and costly, than comparable single-phase equipment, and (3) single-phase generators have been able to provide enough milliamperage to insure adequately short exposure times for routine radiography (2, 33, 65, 67, 103). During the past decade, however, there have been developed certain specialized radiographic techniques, particularly in the field of cardiovascular studies, which require very short exposure times and correspondingly high milliamperages, as well as highly demanding tube operating cycles (34, 41, 74). Since these requirements are most easily accomplished through the use of three-phase generators (67, 75), interest in three-phase equipment has greatly increased in the United States during the past five to ten years (22, 23, 34).

The Appendix lists several of the world's major x-ray equipment companies which are presently marketing three-phase apparatus.

Single- and Three-Phase X-Ray Circuits

Basically, an x-ray tube consists of an electronic filament and a metal target contained within an evacuated envelope. Generation of

x rays is achieved when electrons emitted by heating the filament are accelerated to high energy and strike the target. The electronic circuitry employed to accomplish this consists of a high-voltage[3] section which provides the accelerating voltage, and a control section which adjusts the rate of electron emission and the accelerating voltage attained. Since any difference in the output[4] and quality[4] of x-ray beams produced in a given x-ray tube by single-phase and three-phase generators are due to the differences in waveform of the accelerating voltages (53), the discussion will be limited to the high-voltage circuitry[5].

Single-Phase Circuits

In its simplest form, the single-phase x-ray circuit consists of a high-voltage step-up transformer with its secondary connected to the

---

[3] In this context, "high-voltage" refers to potentials in the order of tens of thousands to hundreds of thousands of volts.

[4] "Output" is a term used to describe exposure rate at a specified point under standardized conditions (43). It is usually expressed in roentgens per minute. The "quality" of an x-ray beam is related to its ability to penetrate matter, which in turn, is dependent upon the energy of the photons which make up the beam. The internationally accepted method for specifying beam quality is to state the half value layer (HVL), that is, the amount of a given material which is required to attenuate the output by one-half (26).

[5] For more detailed discussion of both the low- and high-voltage circuitry used in x-ray generating apparatus, see the following references: (49), (65), (78), and (106).

anode (target) and cathode (filament) of an x-ray tube, as shown in Figure 4. Since the x-ray tube normally will only conduct when the anode is at a positive potential with respect to the cathode, this is called a "self-rectified" circuit.

A short-coming of self-rectified circuits exists in the possibility of heating the tube target to incandescence through excessive operation. When this occurs, electrons, emitted from the overheated target during the time that the anode potential is negative with respect to the cathode, are accelerated towards the filament and may damage it or shorten its useful life. This condition is called "inverse emission". For this reason, self-rectified circuits are only used in low-capacity x-ray apparatus (92).

In order to forestall inverse emission, two rectifiers may be placed in the circuit, as shown in Figure 5. The rectifiers limit tube voltage and current to the positive cycle.

In both of the above described circuits, only one-half of the voltage waveform is used, producing one x-ray pulse per cycle. Thus, they are referred to as "half-wave", or sometimes, "one-pulse" devices.

For purposes of achieving greater output and more uniform target loading, four rectifiers are often used in a "bridge" circuit, as shown in Figure 6. This circuit, which is most commonly used in medium- to high-capacity diagnostic x-ray equipment (92), uses the

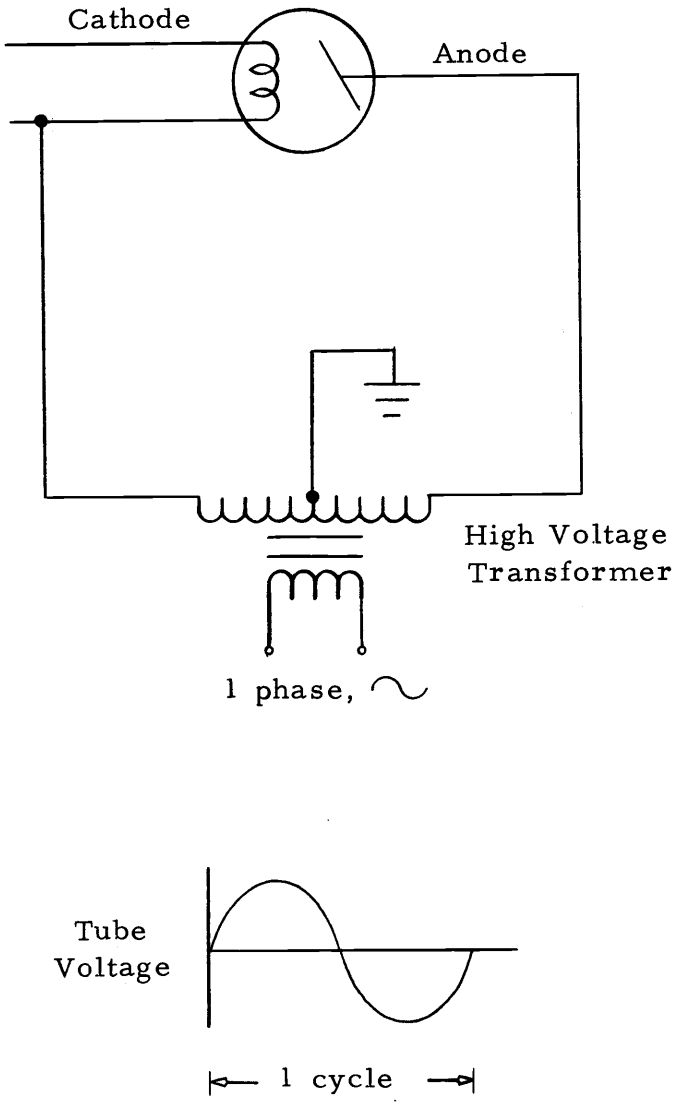

Figure 4. Single-phase, self-rectified x-ray circuit.

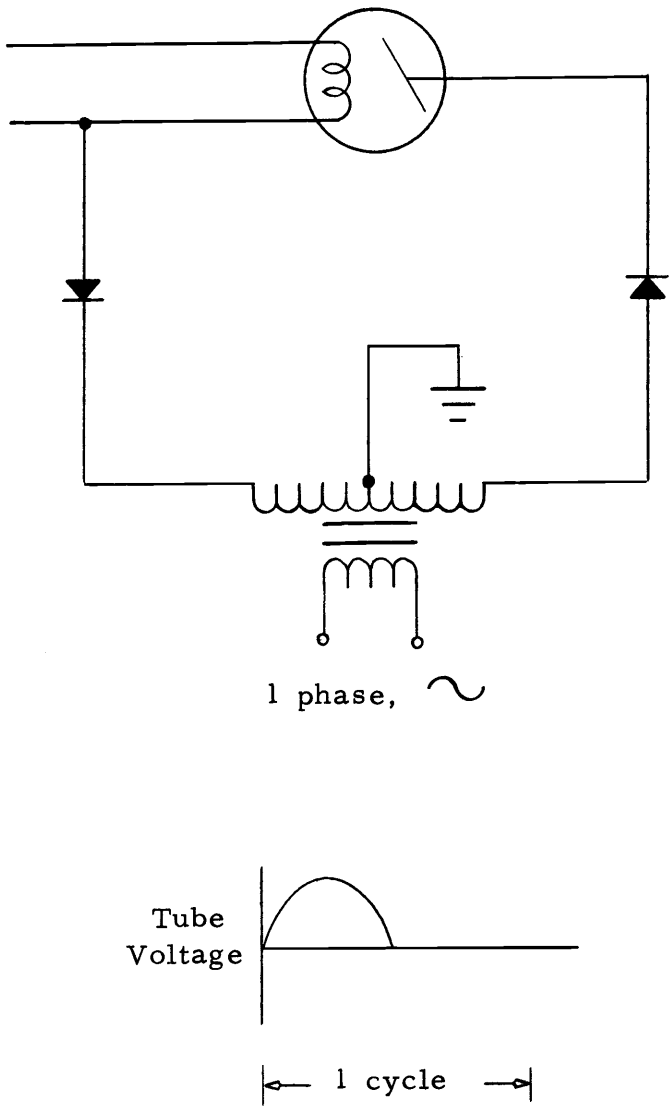

Figure 5. Single-phase, half-wave rectified (one-pulse) x-ray circuit.

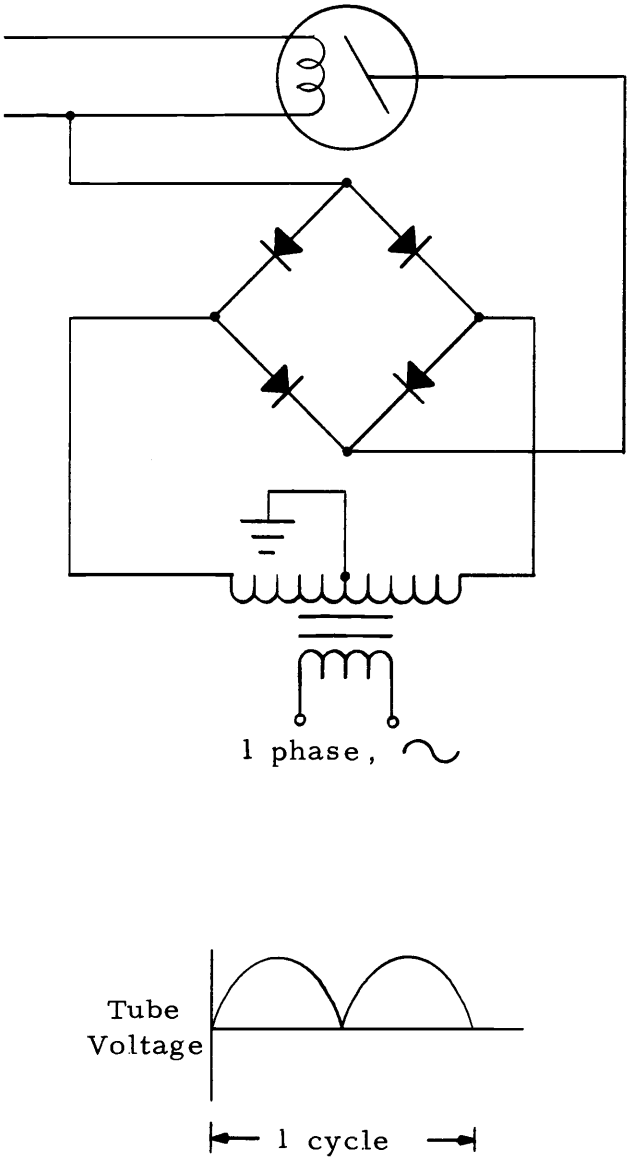

Figure 6. Single-phase, full-wave rectified (two-pulse) x-ray circuit.

full voltage waveform, producing two x-ray pulses per cycle. These are called "full-wave rectified" or "two-pulse" devices.

Three-Phase Circuits

Three-phase transformers have three primary windings and three secondary windings. These windings may be connected in a "star" or "Y" pattern or in a "delta" (Δ) pattern, as shown in Figure 7 (59).

A simple three-phase circuit uses six rectifiers to provide full-wave rectification of each phase. The transformer primary is connected in delta fashion and the secondary is connected in star fashion, as in Figure 8. Since six pulses of x ray are produced for each complete alternating current cycle, this circuit is referred to as "three-phase, six-pulse".

A second type of three-phase x-ray circuit employs 12 rectifiers and 2 three-phase transformers whose outputs are out of phase with each other by 1/12 of one cycle. This phase-shift is accomplished by having the primary of one transformer connected in star fashion and the primary of the other connected in delta fashion. The secondaries of both are connected in star fashion, as in Figure 9.

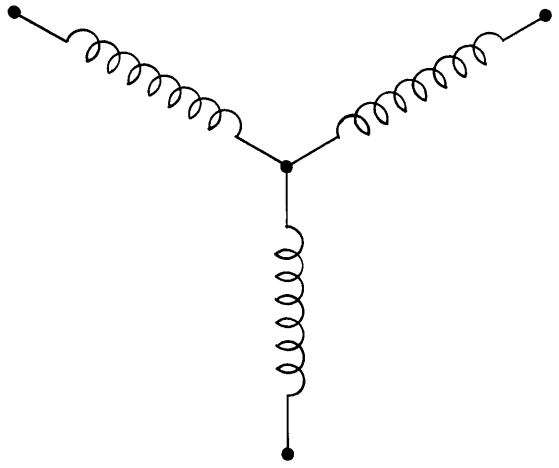

"Star" or "Y"
Winding

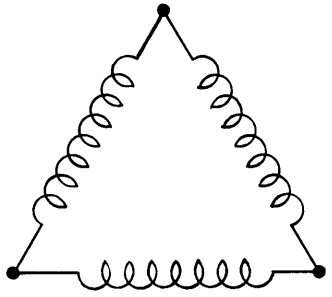

"Delta" (Δ)
Winding

Figure 7. Three-phase transformer windings.

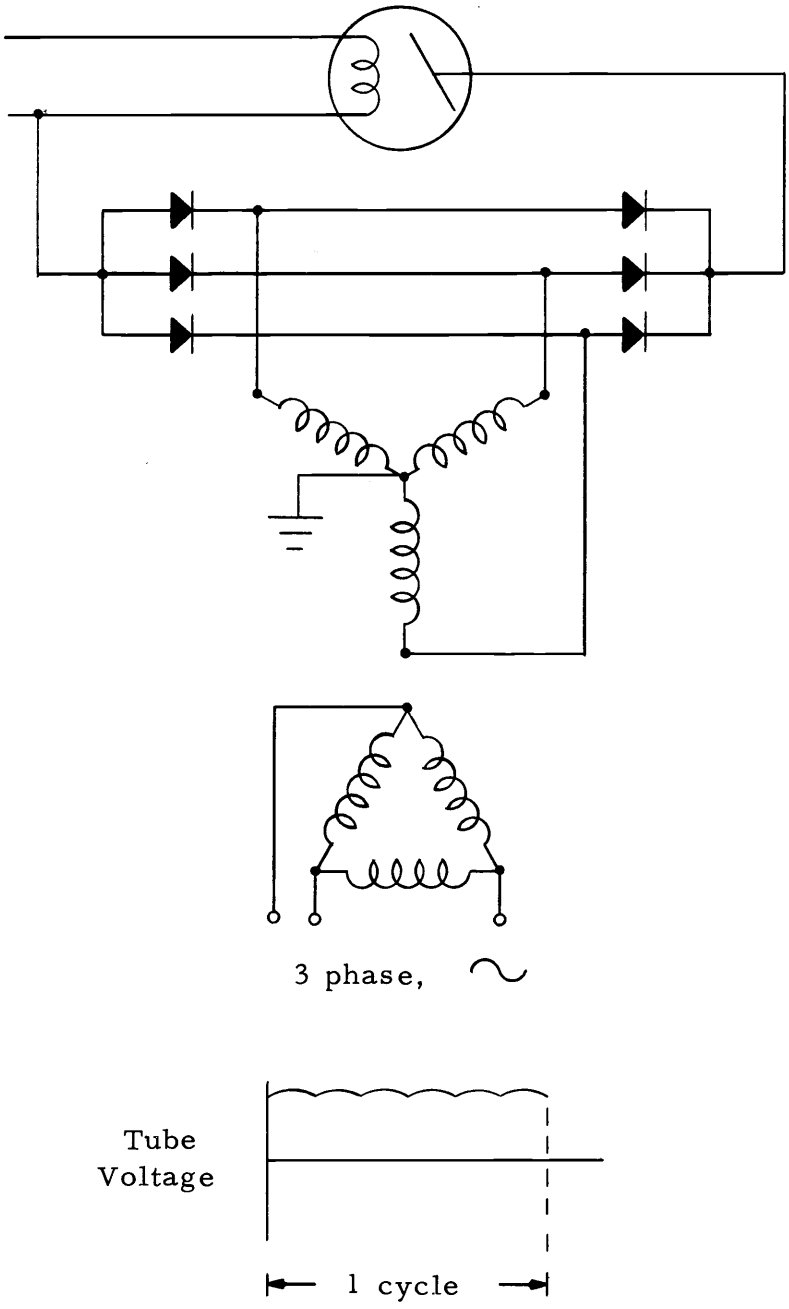

Figure 8. Three-phase, six-pulse x-ray circuit.

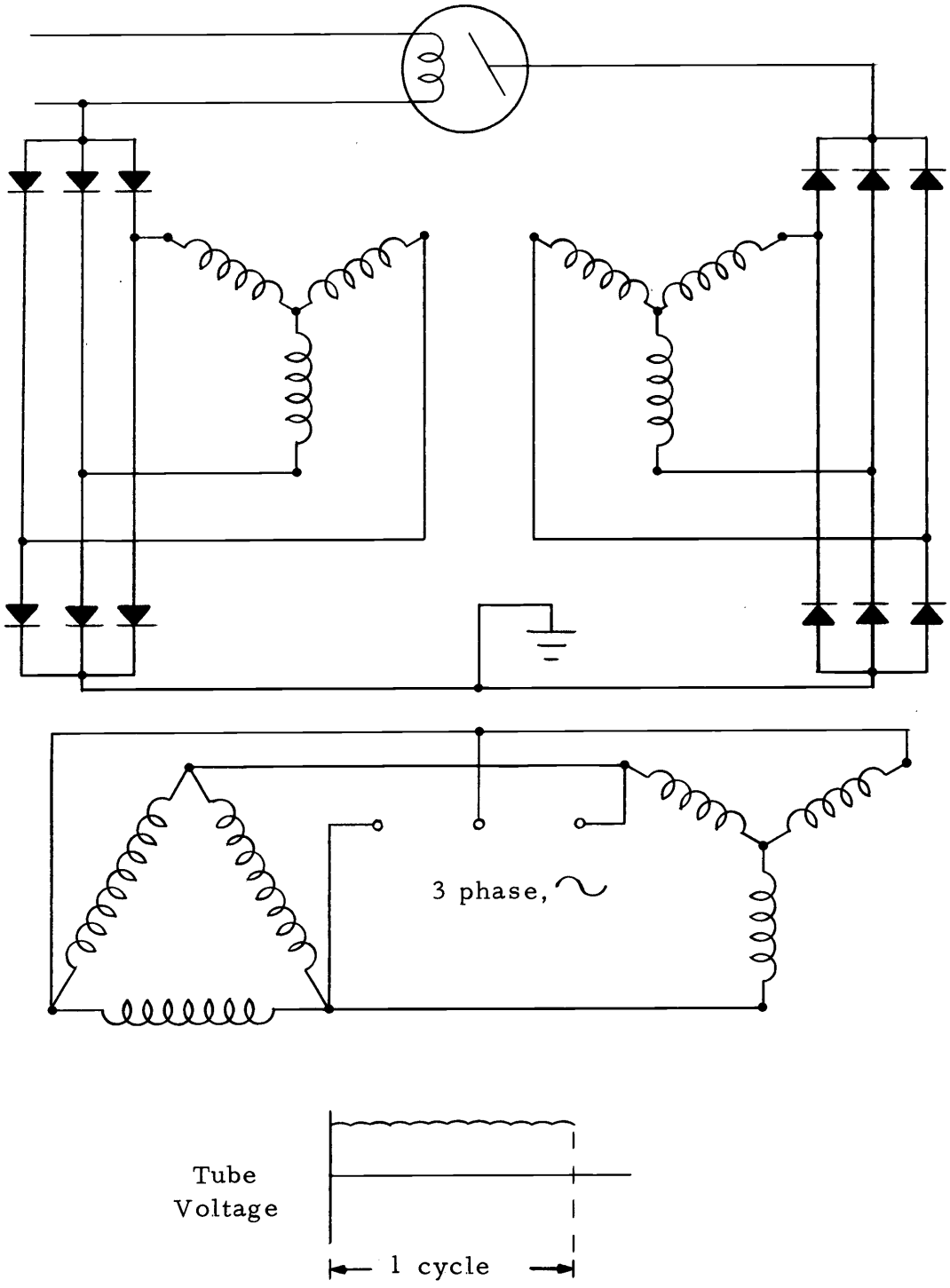

Figure 9. Three-phase, twelve-pulse x-ray circuit.

Comparison of Voltage Waveforms

It was stated above that any differences in output and quality between x-ray beams generated with single-phase and three-phase equipment could be attributed to differences in the waveforms of the voltage across the x-ray tube. Figure 10 shows idealized waveforms for single-phase, two pulse; three-phase, six-pulse; and three-phase, twelve-pulse generators. Obviously, three-phase provides a more uniform voltage. Ripple[6] for 6-pulse and 12-pulse is theoretically 13.5% and 3.4%, respectively (74). However, under load, the waveforms become distorted (78) and the effective values are approximately 20% and 5%, respectively (92)[7]. With single-phase, voltage varies between zero and the peak kilovoltage (kVp), and the ripple is 100%.

It is possible to calculate peak, average, and root-mean-square (rms) tube voltages and currents for single-phase and three-phase generators assuming sinusoidal waveforms. The results are summarized in Table 1 for x-ray generators operating at 100 kVp with 100 mA tube current. The calculations are shown in the Appendix.

---

[6] Voltage ripple is defined as the peak-to-peak variation in voltage (79). Here it is expressed as a percentage of the maximum potential.

[7] The ripple value found in actual practice for any given unit is also determined by the high-voltage cable capacitance which is proportional to cable length.

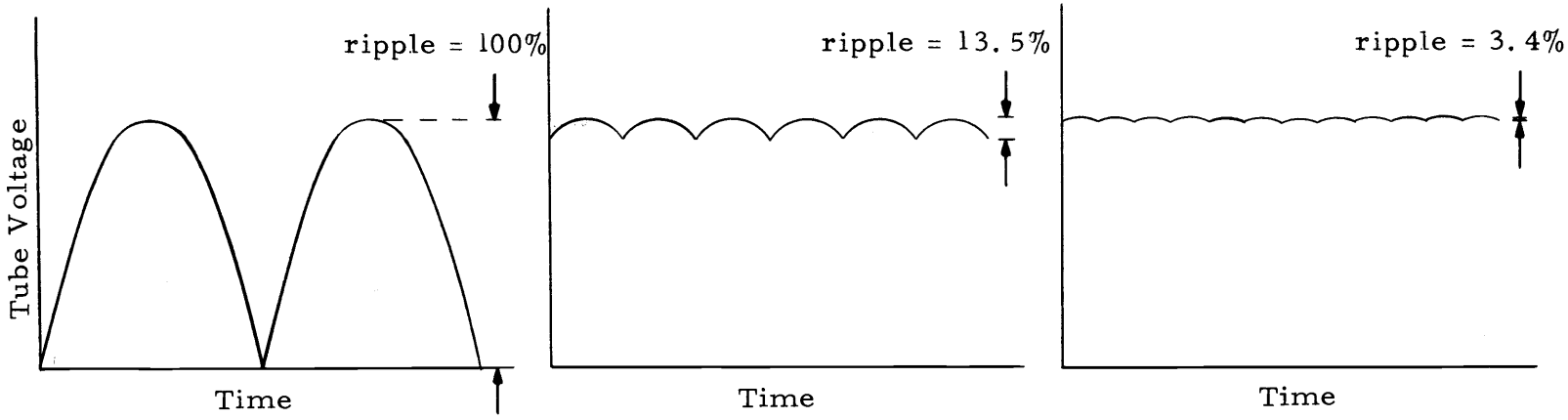

(a) Single-phase
Two-pulse

(b) Three-phase
Six-pulse

(c) Three-phase
Twelve-pulse

Figure 10. Single- and three-phase voltage waveforms.

Table 1. Voltage and current values for generators operating at one hundred kilovolts and one hundred milliamperes.

Generator Type	Voltage (kV) Peak	Avg	Rms	Current (mA) Peak	Avg	Rms
Single-Phase	100	64	71	157	100	111
3-Phase, 6-Pulse	100	95	96	105	100	101
3-Phase, 12-Pulse	100	99	99	101	100	100

(Actual values would be somewhat different due to waveform distortion.)

Influence on X-Ray Beam Quality

An expression derived for the spectral distribution of x-ray photon intensity produced within an x-ray tube target by monoenergetic electrons of energy E° is

$$\begin{aligned} dI &= CZ(E^{\circ} - E)dE, \qquad 0 < E < E^{\circ} \\ &= 0, \qquad\qquad\qquad\quad \text{elsewhere} \end{aligned} \tag{1}$$

where dI is the intensity of photons with energy E, Z is the atomic number of the target, and C is a constant of proportionality (13). This result is in agreement with direct experiments (18).

When electrons of many different energies interact with the target, the overall intensity distribution of the x-ray photons produced is just equal to the sum of the individual distributions, or

$$\begin{aligned} dI &= \sum_i C_i Z(E_i^{\circ} - E)dE, \qquad 0 < E < E_i^{\circ} \\ &= 0, \qquad\qquad\qquad\quad \text{elsewhere} \end{aligned} \tag{2}$$

where E_i° is the i^{th} initial electron energy and C_i is the proportionality constant for the electron group of initial energy E_i. dI, E, and Z are defined as for Equation 1. In effect, C_i is a weighting factor which takes into account the electron distribution, and is directly proportional to the number of electrons having initial energy E_i°.

From the data in Table 1 and the ripple percentages listed above, it is obvious that the electron energy distributions for 3-phase generators are very narrow, with the average electron energy for 6-pulse and 12-pulse being equal to 0.95 $(E_i^\circ)_{max}$ and 0.99 $(E_i^\circ)_{max}$, respectively. For single-phase, however, the electron distribution is quite broad, extending all the way down to zero, with an average electron energy of .64 $(E_i^\circ)_{max}$. Thus, for the same maximum photon energy, x-ray beams generated with single-phase units are not as rich in high energy photons as are those generated by three-phase units (92).

Influence on X-Ray Beam Output

X-ray beam output is greater for three-phase generators than for single-phase generators operated at the same kVp and mA. The reasons for this are two-fold: (1) since the quality of the three-phase x-ray beams is greater, they are better able to penetrate the tube walls and the added filtration placed in the beam, (2) more total x-ray energy is produced by three-phase generators.

The total x-ray energy produced, when a beam of electrons of energy E° interact within an x-ray tube target, may be found by integrating the x-ray intensity over all energies. From Equation 1 above,

$$E_{total} = \int dI$$

$$= \int_{O}^{E^{\circ}} CZ(E^{\circ} - E)dE \qquad (3)$$

$$= \frac{CZ(E^{\circ})^2}{2}$$

Thus, the total x-ray energy produced is proportional to the square of the initial energy of the electrons. Since the average initial electron energy is greater in three-phase, so too will be the total x-ray energy and the beam output.

Influence on Tube Loading

The efficiency of x-ray production may be defined as the fraction F, of the total electron energy incident upon the target which is converted to x-ray energy or, from Equation 3 above,

$$F = \frac{E_{total}}{nE^{\circ}}$$

$$= \frac{CZ(E^{\circ})^2}{2nE^{\circ}}$$

where n is the number of electrons which strike the target. Since the constant C varies linearly with n, (total x-ray energy produced is directly proportional to the number of incident electrons), the term C/2n may be taken as a new constant, k. Thus,

$$F = kZE^{\circ} \qquad (4)$$

The value of k has been found to be 0.9×10^{-6} where E° is expressed in keV (5). Thus, for a typical tungsten target x-ray tube operating at 100 kVp, the efficiency of x-ray production is only 0.007. More than 99% of the electron energy is converted to heat, which limits the tube loading[8]. Exposure factors (kVp, mA, time, number of exposures) must be restricted so that none of the various tube-housing components becomes overheated.

Most radiography today is performed with x-ray tubes which have a rotating anode, in order to spread the area of electron bombardment over a larger target area (65). With 60 Hz alternating current frequency, the typical anode rotation speed is 3000 - 3600 rpm (78), or approximately 1 revolution per 0.02 seconds. Obviously, for single exposures of 0.02 seconds or less, no area of the target will be exposed more than once.

For these short exposures, the surface temperature of the anode is the limiting factor (65) and is determined by the peak power input to the tube. However, with single-phase, the target loading is not uniform but varies from zero to maximum as do both the voltage and current waveforms. Using the data in Table 1 for equipment operating at

---

[8] Tube loading is generally expressed in terms of "heat-units" (HU). 1 HU = 1 kVp x mA x sec x W. W, a factor which takes into account the waveform of the voltage, is taken as 1 for single-phase, and 1.25 for three-phase generators (24). One HU is approximately equal to 0.2 calories.

100 mA and 100 kVp, the peak power input (equal to peak voltage times peak current) to a target for single-phase is 15.7 kVA. For three-phase, the peak power input is only 10.5 kVA. Thus, for short exposures on a given tube, it would be possible to increase the product of kVp x mA by more than 50% using three-phase rather than single-phase. It should be noted that the tube rating is independent of exposure time in this region of operation.

For long exposures or for a series of short exposures, the temperature of the x-ray tube-housing taken as a whole (tube envelope, insulating oil, high-voltage cable terminals, etc.) becomes the limiting factor and is determined by the average heat-input to the tube and the tube cooling characteristics. Heat-input is proportional to effective (rms) voltage times effective current. For the same kVp and mA, the ratio of three-phase heat-input to that for single-phase is calculated to be approximately 1.25. This ratio is, in fact, identical to the factor "W" in Footnote 6 above.

Thus, the advantage of a higher three-phase tube rating steadily decreases with increasing exposure time. The ratio of the three-phase rating to that for single-phase varies from 1.5 to 0.8. In the transition region of intermediate length exposure (0.1 to 1.0 sec), the temperature of the anode structure is the limiting factor (65).

Influence on Minimum Exposure-Time

The most important advantage, that is claimed for three-phase x-ray equipment over single-phase, is the ability to obtain a given radiographic result in a shorter exposure-time (41, 52, 74, 75, 103). This may be considered from three standpoints:

1. Comparing equipment operating at the same kVp and mA. In this case, the decreased exposure-time is due to the greater beam quality (penetrating power) and the greater beam output of three-phase equipment.

2. Comparing equipment operating at different kVp and mA. It has been claimed that a single-phase beam could be made equivalent to a three-phase beam by merely raising the kVp sufficiently to compensate for the difference in quality and output (34, 75). Although two such beams could never be exactly equivalent due to the difference in generating voltage waveform, it may be assumed, for practical purposes, that this claim is correct. It is also assumed that the maximum possible mA, consistent with the tube rating, would be used for minimum exposure-time. However, as shown above, the tube ratings are independent of time for exposures less than 0.02 seconds. For these short exposures, therefore, raising the kVp necessitates lowering the mA in order to hold the product of kVp x mA constant. This decrease in mA requires a corresponding increase in exposure-time.

On the other hand, for short exposures with three-phase equipment, it is possible to use, with the same tube at a given kVp, an mA value approximately 50% higher than is allowed for single-phase. This mA increase allows a corresponding decrease in exposure-time. Thus, the three-phase equipment will still provide the shortest exposure-time.

3. Comparing the minimum available exposure-time setting. Typically, the minimum exposure-time setting for a three-phase unit is 0.003 seconds; that for a single-phase unit is 1/120 or 0.0083 seconds, corresponding to one pulse. However, in single-phase, the major portion of the radiation intensity is emitted during the central half of the voltage pulse or within approximately 0.004 seconds (33, 92). For three-phase, the elapsed time is essentially equal to the radiation time. Therefore, at the minimum available time settings, there is only a 33% actual increase in exposure time in going from three-phase to single-phase.

If, however, the exposure is such that the next higher exposure-time setting is required, the actual time difference increases to 105%. This is because the next single-phase timer-setting is 2 x .0083 = .0166 seconds. The actual elapsed time from the start of the first radiation pulse to the end of the second pulse is .0166 - .0043 = .0123 seconds. The corresponding three-phase timer setting is 2 x .003 = .006 seconds.

The time differential continues to increase approaching 170% at exposure time settings of .083 seconds and .03 seconds for single-phase and three-phase, respectively.

Purpose of This Study

In the energy range used in diagnostic radiography, the x-ray absorption coefficient is inversely proportional to photon energy. Therefore, most of the lower-energy photons are preferentially absorbed within the patient and do not contribute to the exposure of the film (94). Since x-ray beams generated by three-phase apparatus contain a lesser proportion of lower-energy photons than those generated by single-phase units, it has been claimed that use of three-phase generators would result in a lower patient dose per film exposure (70). It is the purpose of this study to measure and compare the dose distributions within a phantom exposed under conditions resembling those used in diagnostic radiography.

II. EXPERIMENTAL TECHNIQUE

X-Ray Apparatus

The output and quality of an x-ray beam are affected by many factors. These include kVp, mA, total filtration in the beam, distance from the source to the point of observation, and the voltage waveform. The voltage waveform is determined by the generator phase, type of rectification, and the capacitance of the high-voltage cables (3, 67, 99). In this study, in order to isolate effects due only to phase differences, both the single-phase and three-phase generators used, had the same type of rectifiers, and were connected to the same tube-housing assembly by means of the same set of high voltage cables.

The single-phase generator[9] used, was a full-wave unit rated at a maximum voltage of 150 kVp and a maximum current of 300 mA. The three-phase generator[10] was a 12-pulse unit with maximum ratings of 150 kVp and 700 mA. The generators were alternately connected to a rotating anode x-ray tube[11] with 30 foot high-voltage cables. Target angle was 17 1/2 degrees and nominal rotation speed was 3200

---

[9] Model DXS 350 X-Ray Unit manufactured by General Electric Medical Systems Department, Milwaukee, Wisconsin.

[10] Model DXR 750-II X-Ray Unit manufactured by General Electric Medical Systems Department, Milwaukee, Wisconsin.

[11] General Electric Model HDN

rpm. The total filtration of the tube unit and adjustable collimator was equivalent to three millimeters of aluminum which exceeds the minimum recommended by the National Council on Radiation Protection and Measurements (68).

The kilovoltage was calibrated with a resistance divider which samples 1/1000 of the total tube potential. The voltage waveforms were displayed and measured on a dual trace oscilloscope[12] with memory and voltage calibration modules. The absolute kVp error was estimated to be less than $\pm 5\%$ and the kVp agreement between the two generators was estimated to be within $\pm 3\%$. The tube current, which was read by means of the same milliameter externally connected to each of the generators, was maintained at 100 ± 2 mA.

Choice of Dosimeters

Thermoluminescent dosimeters (TLD's), rather than ionization chambers, were chosen to measure exposures within the phantom. The primary objection to using ion chambers for these measurements is the error which results from the insertion of an air volume within the phantom material. This causes both an increase in the measured exposure due to decreased attenuation of the primary and scattered radiation, as well as less actual exposure adjacent to the chamber due

---

[12] Model 564 manufactured by Tektronix Inc., Portland, Oregon.

to the loss of scattered radiation from the displaced material (12, 76). Measurements of these errors have been made for x rays of 80 to 150 kVp and have been found to be as large as 15 percent, depending upon chamber size, depth in the phantom, and radiation quality (1, 56, 73).

Since the lithium fluoride TLD's used in this project are very small (rods, 1.25 mm diameter by 6.5 mm long) and since they have nearly the same energy absorbing qualities as tissue (21, 49), errors due to material displacement are negligible. Other problems associated with the use of chambers, such as scatter losses due to shielding by heavy metal stems (66, 71, 76), dose rate dependence (96), and errors due to large dose gradients (96), are not applicable to these dosimeters.

Another advantage of using TLD's in this study was that many dosimeters could be placed within the phantom at one time and data for a complete dose distribution curve could be obtained with one exposure rather than making seperate exposures for each depth-dose measured[13]. This technique has greater precision since any contribution to within-curve variance due to variability in x-ray machine output is eliminated.

---

[13] The effects of dosimeter "stacking" are discussed in the section on "Dosimeter Arrangement".

General Theory of Thermoluminescent Dosimetry

The use of thermoluminescent (TL) media for radiation dosimetry has been well investigated and reported. Five hundred and six references pertaining to this subject have been compiled by Lin and Cameron (57) and an additional one hundred and seventy-two have been listed by Spurney (88).

Though the chemical and physical theory of thermoluminescence is not completely known, the basic phenomenon is qualitatively understood (10). Ionizing radiation interacting with a TL crystal raises electrons from the valence band to the conduction band, leaving behind holes. The electrons and holes are then free to move through the crystal until they recombine or are trapped at impurities or other imperfections in the crystal lattice. Heating of the crystal releases the trapped electron-hole pairs, which then recombine and release the stored excitation energy in the form of a photon of light (Figure 11).

The temperature required to release the trapped electrons is a function of the trap depth. As the crystal is heated, the probability of releasing any particular electron increases until at some temperature, it becomes virtually one hundred percent. Thus, the light emitted will increase in intensity, reach a maximum, and then return to zero. The plot of this light as a function of temperature (or heating time) is called a glow-curve.

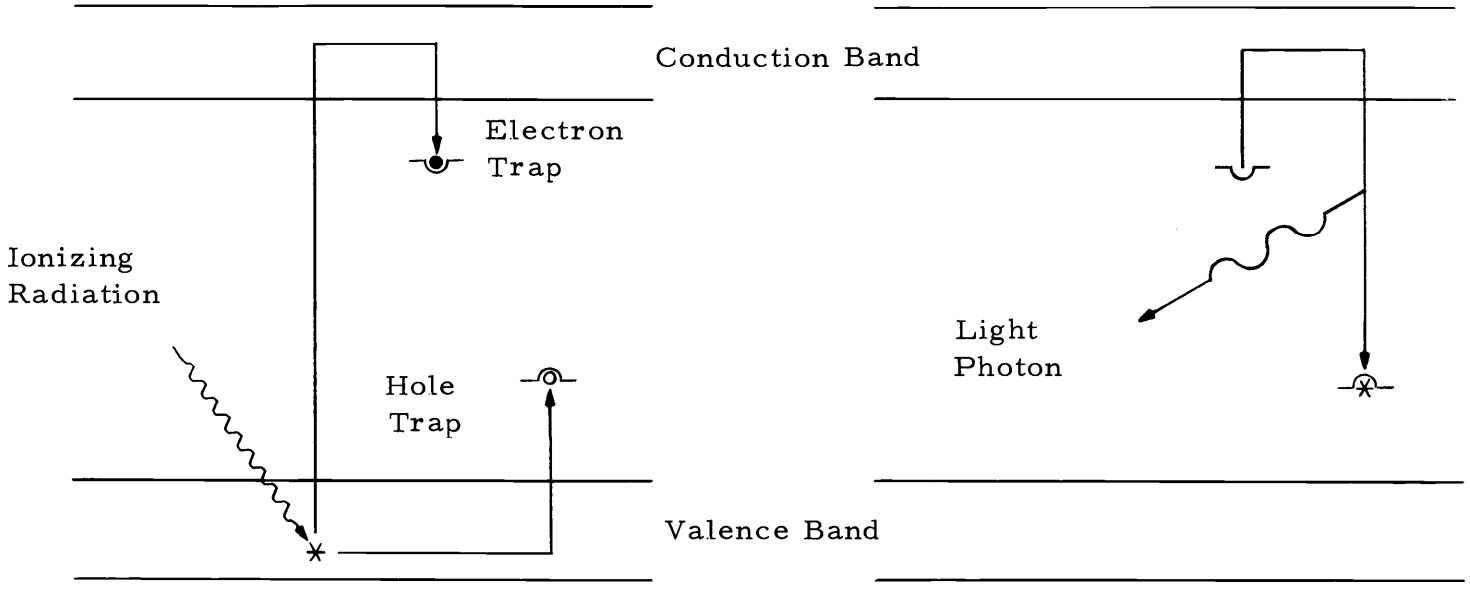

(a) Exposure to ionizing radiation

(b) Release of stored energy by heating

Figure 11. Energy-level diagram of a crystal exhibiting thermoluminescence due to ionizing radiation.

If the TL material has only one trap depth, then it will exhibit only one glow-curve peak. Manganese activated calcium fluoride (CaF_2:Mn) is an example of this type (25, 82). On the other hand, some TL materials, such as lithium fluoride (LiF), have several trap depths and therefore several glow-curve peaks associated with them (90, 107).

The dose absorbed by the thermoluminescent dosimeter (TLD) is proportional to the total amount of light emitted upon heating. This may be measured by integrating the glow-curve. However, if the heating rate is held constant, it is necessary only to read the peak of the glow-curve, since this also will be proportional to dose. Readout systems of both types have been designed and are presently in use (8). The reader[14] used in this project provides complete glow-curves with a constant heating rate enabling peak-height measurement. An example of a typical glow-curve readout is shown in Figure 12.

Characteristics of Lithium Fluoride Phosphor

The characteristics of LiF make it quite suitable for depth-dose dosimetry. It has an effective atomic number of 8.14 compared to 7.42 for that of tissue and 7.62 for that of air (45, 62). It is inert,

---

[14] Model TL-3B Thermoluminescent Dosimeter Reader manufactured by Edgerton, Germeshausen and Grier, Inc., (EG&G), Goleta, California.

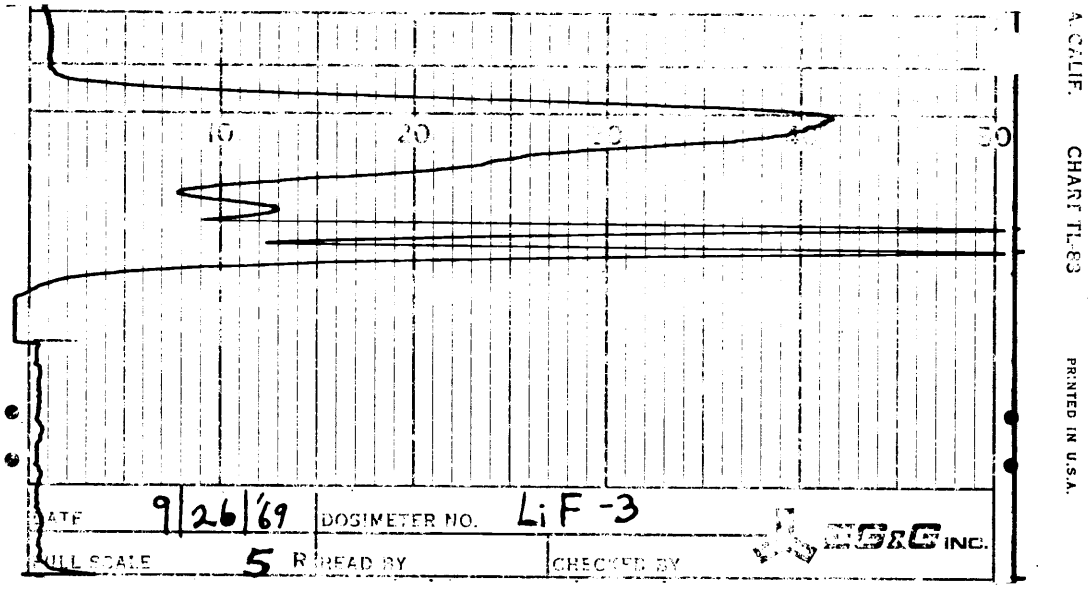

Figure 12. Glow-curve readout of a lithium fluoride thermoluminescent dosimeter.

insoluble, non-toxic, and stable in air (10). The five glow-peaks associated with it have half-lives at room temperature of five minutes, ten hours, one-half year, seven years, and eighty years (107).

Prior to exposure, the phosphor is returned to ground state by annealing to remove any trapped electrons. The generally specified regimen for this is 1 hour at 400° C followed by 24 hours at 80° C (8, 11, 36, 107). The 24 hours at 80° C essentially removes the first two low-temperature glow-curve peaks, thereby reducing the problem of fading between exposure and readout (8, 36, 107). Since, in this study, only the height of the high-temperature peak was read, low-temperature annealing was unnecessary. LiF read out in this manner has been found to exhibit very little fading (9, 10, 54, 69, 89, 90, 105).

Repeated annealing cycles have not been shown to alter its sensitivity (37, 60) and response is independent of humidity (36) and temperature during irradiation between -50° C and 100° C (28).

The useful range of LiF dosimeters is from a few mR to greater than 10^9 R (15, 27, 62, 69). No dose-rate dependence has been observed over this entire range for dose-rates from less than 0.1 R/sec to 10 R/sec (16, 54, 62, 69, 93). However, response is only linear up to approximately 1000 R, beyond which, sensitivity increases, and it becomes supralinear (15, 72, 84, 101).

LiF is only slightly energy dependent, as would be expected, since its effective atomic number is quite close to that of air. Response at 30 keV is approximately 30 percent greater than that at 1.25 MeV (9, 10, 11, 55, 100).

Energy Calibration

Hendee et al (39) have shown that the increased LiF response at low photon energies causes a displacement of percent depth-dose curves from those measured with ionization chambers. Therefore, a means was devised to correct for the energy dependence of the LiF and at the same time to monitor the quality of the x-ray beam as a function of depth in the phantom. CaF_2:Mn has an effective atomic number of 16.5 and its response at 30 keV is about 13 times that at 1.25 MeV (8, 25). Thus the ratio of CaF_2:Mn response to LiF response is a function of beam quality and may be used in conjunction with a LiF energy-response curve to correct the LiF measurements.

Similar techniques for beam quality measurements have been reported in the literature; Kenney and Cameron (55) have used a mixture of LiF and Al_2O_3 powder; Facey (19) has used LiF and $CaSO_4$:Sm; and Gorbics and Attix (28) have used tandem dosimeters of LiF and CaF_2:Mn read out simultaneously.

CaF_2:Mn is quite similar to LiF in its pertinent phosphor characteristics; it exhibits little fading (20, 81), it is linear over its entire

useful range which extends from a few mR to over 10^5 R (20, 60, 81, 84), it is dose rate independent from less than 10^{-2} mR/sec to 10 R/sec (20, 81, 93), and its response is independent of temperature up to 150° C during irradiation (29). The dosimeters used in this study are sealed glass ampoules, 0.9 mm in diameter by 6 mm long containing approximately 0.8 mg of CaF_2:Mn phosphor.

Choice of Phantom Material

In order for different materials to have closely similar x-ray scattering and absorbing properties, they must have nearly the same (1) atomic number, (2) mass density, and (3) electron density (86). For muscle tissue, the respective values are: 7.42, 1.0 g/cm^3, and 3.36×10^{23} electrons/g (86).

The common material which comes closest to tissue in these properties is water, which has the following corresponding values: 7.42, 1.0 g/cm^3, and 3.34×10^{23} electrons/g (65). Since water is readily available with constant composition and is low in cost, it is often used as the material of choice for radiation dosimetry. However, in this study, a solid material was required to serve as a support matrix for the thermoluminescent dosimeters used.

In addition to the physical properties listed above, a solid phantom material should be available in sheets so that incremental changes in thickness can be conveniently made (35, 58). Dry

pressed-woods, such as Masonite or "hardboard", have been used for this purpose. However, it has been found that these do not absorb x rays in the same manner as water (3) and are not suitable as phantom material for energies below 200 keV (6).

Several wax mixtures containing mostly paraffin wax with additives of beeswax, resins, or other materials have been tried (65). Of these, a mixture described by Jones (51) called "Mix D", is the most nearly equivalent to tissue (35, 47) and is recommended for use as a phantom material by the International Commission on Radiological Units and Measurements (ICRU) (43).

Mix D, which was used in this study, is commercially available[15] in 30 x 30 cm sheets, nominally 1 cm thick. It is composed of 60.8 percent paraffin, 30.4 percent polyethylene, 6.4 percent magnesium oxide, and 2.4 percent titanium dioxide (all percentages by weight). It has an effective atomic number of 7.47, a density of 0.99 g/cm^3, and an electron density of 3.36×10^{23} electrons/g. Depth dose and scatter measurements made with Mix D differ from those made with water by less than three percent over the energy range from 18 keV to 78 keV (51).

---

[15] From Astor, Boisselier and Lawrence Ltd., London, England.

III. EXPERIMENTAL PROCEDURE

Dosimeter Calibration

Normalization of LiF and CaF_2:Mn Dosimeters

Twenty dosimeters of each of the LiF and the CaF_2:Mn type were available for this study. The LiF dosimeters were in the form of hot-pressed rods, 1.25 mm in diameter by 6.5 mm long, each containing approximately 21 mg of natural LiF. The CaF_2:Mn dosimeters were glass ampoules, 0.9 mm in diameter by 6 mm long, each containing approximately 0.8 mg of phosphor.

The annealing procedure used throughout this study was as follows:

The dosimeters were inserted in a 7 x 5 x 0.5 cm aluminum block which had been drilled with 20 pairs of 4 mm deep holes, shown in Figure 13. The block was then placed in a pre-heated 400° C oven[16]. At the end of one hour, the block was removed from the oven and placed on a thick aluminum heat-sink which allowed cooling to room temperature in approximately 15 minutes. Uniform cooling conditions are important since the dosimeter sensitivity has been shown to be somewhat affected by changes in cooling rate (8, 37, 107).

---

[16] Type 1400 Furnace manufactured by Thermolyne Corp., Dubuque, Iowa.

Figure 13. Aluminum block used for annealing TL dosimeters. In front of annealing block are shown a LiF dosimeter (left) and a CaF_2:Mn dosimeter.

Figure 14. Styrofoam block used to hold TL dosimeters for calibration exposures.

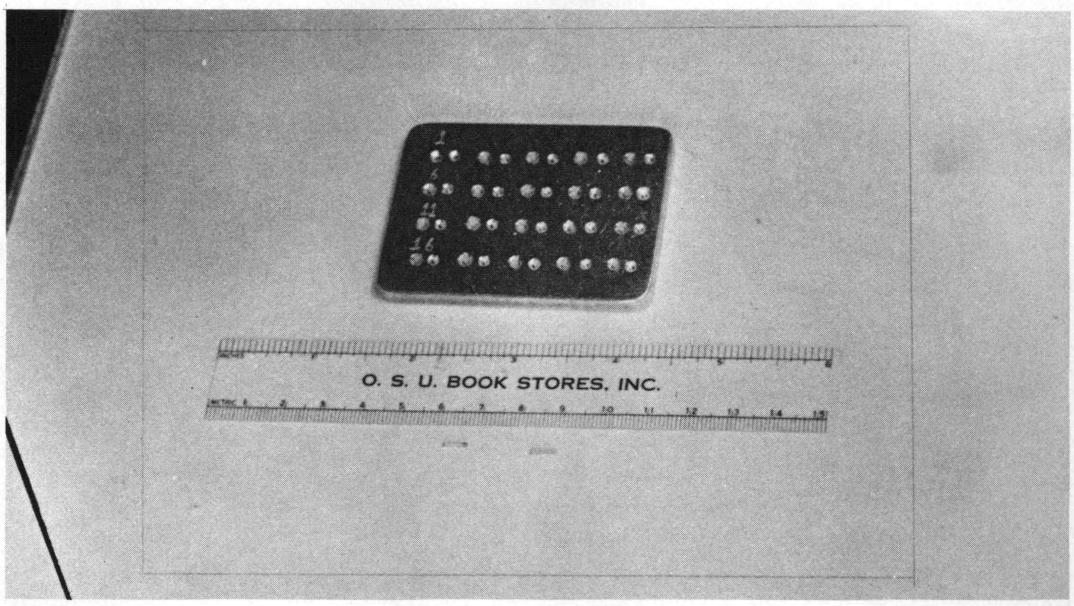
O. S. U. BOOK STORES, INC.

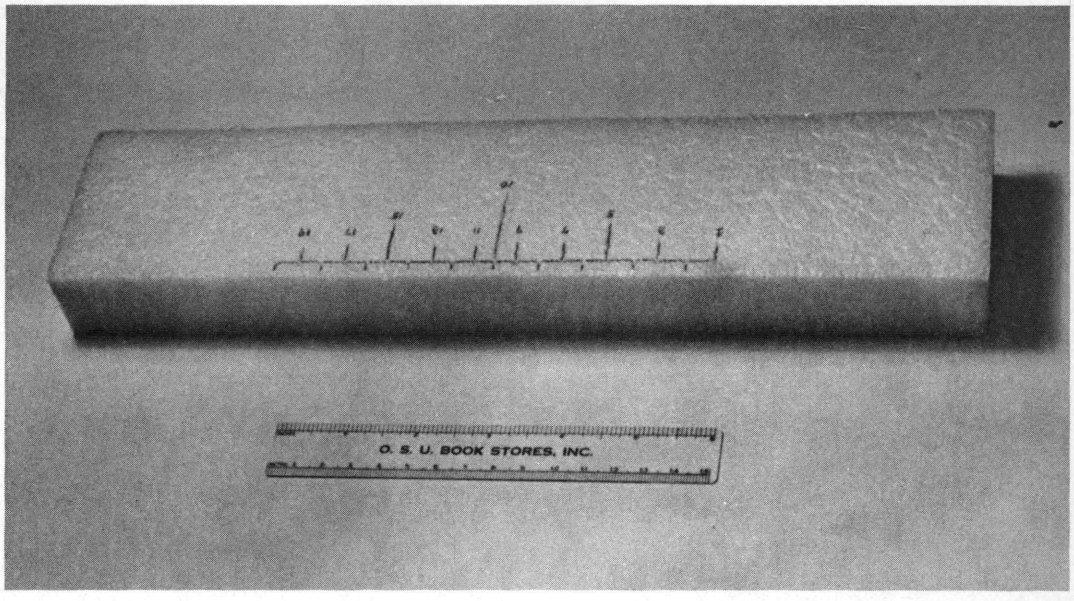
O. S. U. BOOK STORES, INC.

Cameron (8) believes a 10-20 minute cooling time from 400° C to be optimum.

A styrofoam block 3 x 8 x 33 cm was used to support the dosimeters for calibration. Twenty holes were drilled on 8 mm centers along a line parallel to, and 6 mm from the edge of the block placed nearest the x-ray machine (Figure 14). The hole positions were numbered consecutively from one to twenty and the LiF dosimeters were inserted with dosimeter number one in hole number one, dosimeter number two in hole number two, etc. (Although neither the LiF nor the CaF_2:Mn dosimeters are individually numbered, identification is maintained through proper placement in numbered-hole storage cases.)

The x-ray unit[17] used for the dosimeter calibrations was capable of continuous operation at tube voltages from 70 to 300 kVp and tube currents up to 20 mA. The ability to make exposures over extended periods of time eliminated exposure measurement errors due to excessive exposure rates and non-reproducibility of timing intervals.

Exposures were measured with an integrating ratemeter ionization chamber[18]. Two air-equivalent plastic-wall probes were used: Model 10 LA low energy chamber for x rays of effective energy less

---

[17] Maxitron 300 X-Ray Therapy Unit manufactured by General Electric Medical Systems Dept., Milwaukee, Wisconsin.

[18] Model 555 Radocon II Integrating Ratemeter manufactured by the Instrument Division of Victoreen, Inc. Cleveland, Ohio.

than 30 keV, and Model 1 MA medium energy chamber for x rays of effective energy equal to or greater than 30 keV. Correction factors supplied by the manufacturer for these chambers were obtained by intercomparison with instruments whose calibrations are traceable to the U. S. National Bureau of Standards and are accurate to within $\pm$ 3%.

The dosimeters were exposed at 150 kVp and 20 mA with a total filtration of 3 mm of aluminum equivalent. Two minutes yielded an approximate exposure of three roentgens. The field size at the dosimeters was 50 by 50 cm with a source-dosimeter distance (SDD) of 240 cm.

A long SDD was chosen to decrease the angle subtended by the dosimeter array in order to minimize variations in beam intensity. Beam uniformity was checked by exposing a radiographic film in place of the dosimeters and measuring the variations in photographic density. There was less than one percent difference in exposure between any two dosimeter positions.

The dosimeters were read out and the mean reading was determined. Multiplicative factors were then calculated to normalize each dosimeter reading to the mean. This procedure was replicated three times. However, the arrangement of dosimeters was altered each time by choosing at random, the number of the dosimeter which was placed in position number one. The remaining dosimeters were then

inserted in consecutive order. The same procedure was followed using the CaF_2:Mn dosimeters.

The means of the three normalization factors derived for each of the dosimeters are shown in Table 2. The standard errors of the normalized LiF and CaF_2:Mn readings were found to be 3.6% and 4.2%, respectively. These figures are consistent with the findings of Becker (4), Palmer (72), and Svarcer (91).

Linearity Tests

In order to check the linearity of the overall dosimetry system, a series of exposures was made covering the range from 20 mR to 90 R. Twelve each of the LiF and CaF_2:Mn dosimeters were exposed to x rays at 140 kVp with a total filtration of 1.35 mm of Al and 0.68 mm of Cu. Three additional dosimeters of each type were used as zero-exposure controls. Linear regression lines, fitted to the data by means of least squares analysis, are shown in Figure 15. The slopes of the fitted lines for LiF and CaF_2:Mn are 0.997 and 0.992, respectively.

Energy Calibration

Measurements of unique half-value-layer, as described by Trout et al (99), were made at a source-chamber distance (SCD) of 200 cm for effective energies from 18 keV to 140 keV. Effective

Table 2. Normalization factors for thermoluminescent dosimeters.

LiF Dosimeters		CaF_2:Mn Dosimeters	
No.	Factor	No.	Factor
1	1.08	1	.93
2	1.04	2	.97
3	1.00	3	.97
4	1.05	4	.98
5	1.05	5	.97
6	.94	6	1.02
7	1.01	7	1.01
8	.98	8	.99
9	1.02	9	.95
10	.96	10	1.06
11	.96	11	.93
12	.97	12	1.00
13	.96	13	1.01
14	1.01	14	.96
15	1.01	15	1.08
16	1.01	16	1.02
17	.97	17	1.04
18	1.00	18	.95
19	.98	19	.99
20	.97	20	.99

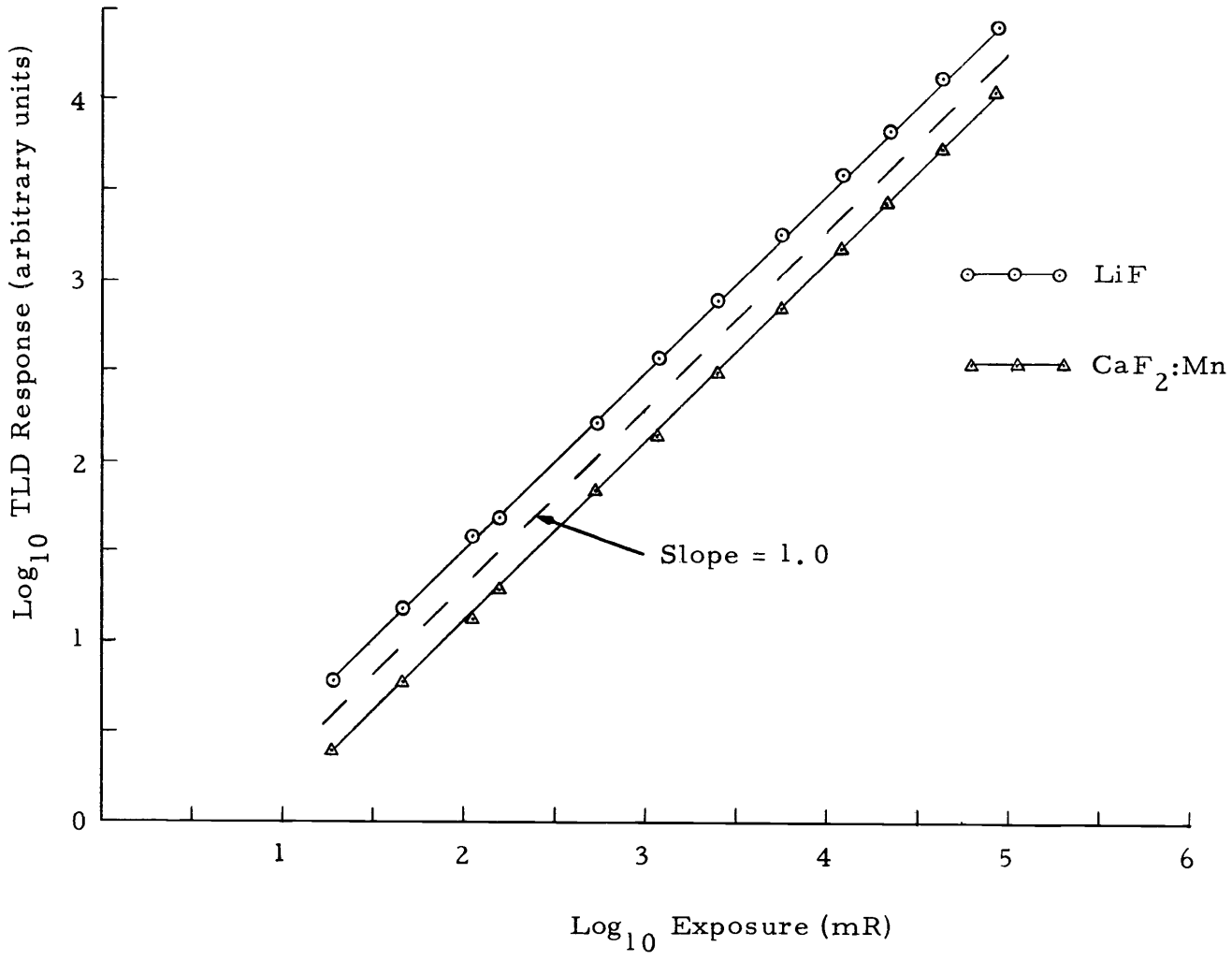

Figure 15. Response of calcium fluoride and lithium fluoride dosimeters vs. x-ray exposure.

energies were calculated using the linear attenuation coefficients determined by Grodstein (32) and McGinnies (63). Kilovoltages, filtration, half-value-layers, and corresponding effective energies are shown in Table 3.

After annealing for one hour at 400 °C, 16 pairs of dosimeters were formed: LiF number one with CaF_2:Mn number one, etc. A different dosimeter pair was then exposed in the styrofoam block, at a SDD of 200 cm, for each different effective energy.

A systematic random sampling procedure was used to select which LiF - CaF_2:Mn dosimeter pair would be used for each calibration energy. A number between one and sixteen was randomly chosen to select the dosimeter pair to be used for the lowest energy calibration. The remaining dosimeters were then used in consecutive order for increasing energy calibration points. This procedure was replicated five times choosing a different random number each time.

Exposures, which were in the order of 10 R, were measured with the ionization chambers described above. Chamber readings were corrected for energy dependence, temperature, and barometric pressure. TLD readings were normalized using the factors in Table 2. The mean LiF response and CaF_2:Mn response per unit exposure were calculated for each energy. From these data, the ratio of CaF_2:Mn response to that of LiF was derived. These response ratios are listed in Table 4 and are shown plotted as a function of effective

Table 3. Energy calibration data.

kVp	Total Filtration mm Al	mm Cu	Unique HVL	Effective Energy (keV)
100	0.35	0	0.575 mm Al	18
100	0.48	0	0.825	20
100	0.73	0	1.23	23
100	1.25	0	1.63	26
100	1.47	0	2.07	28
140	1.60	0	3.10	32
140	3.67	0	5.10	39
140	4.49	0	6.30	44
140	5.74	0	0.33 mm Cu	51
140	1.35	.38	0.56	62
140	1.35	.68	0.73	69
200	1.35	.50	0.97	76
200	1.35	1.15	1.33	87
300	1.35	.75	1.71	96
300	1.35	1.75	2.66	120
300	1.35	4.00	3.53	140

Table 4. Thermoluminescent dosimeter response as a function of x-ray beam effective energy.

Effective Energy (keV)	Response Per Unit Exposure		Relative Response
	LiF	CaF_2:Mn	CaF_2:Mn/ LiF
18	.334	.184	.549
20	.353	.199	.566
23	.361	.220	.606
26	.363	.241	.664
28	.360	.241	.671
32	.353	.214	.607
39	.343	.193	.559
44	.348	.191	.548
51	.335	.176	.521
62	.331	.148	.443
69	.315	.123	.392
76	.320	.106	.324
87	.317	.082	.259
96	.306	.073	.238
120	.293	.047	.162
140	.294	.033	.112

energy in Figures 16 and 17. Included in these figures are the standard errors about each data point.

Depth Dose Measurement

Dosimeter Arrangement

The ICRU recommends that phantoms used for dosimetry be 30 x 30 cm in cross-sectional area and at least 20 cm in depth (43). For the phantom used in this study, 30 x 30 cm sheets of Mix D, which had been machined to a thickness of 1 ± 0.05 cm, were stacked to a depth of 25 cm. Both sides of the sheets were milled to insure close fitting surfaces.

Two grooves were carved into the surface of 20 of the sheets to accept a LiF and a CaF_2:Mn dosimeter, as shown in Figure 18. In assembling the phantom, the orientation was such that the grooves in adjacent sheets were at right angles to each other. Thus, dosimeters directly above each other were separated by a minimum of two centimeters of Mix D.

Trial exposures were made to determine if the dosimeters, stacked above each other in this manner, would cause interference with each other. The Maxitron 300 x-ray unit was used for this purpose and the incident exposures to the phantom were monitored with the integrating ratemeter. Exposures were measured at depths of 5,

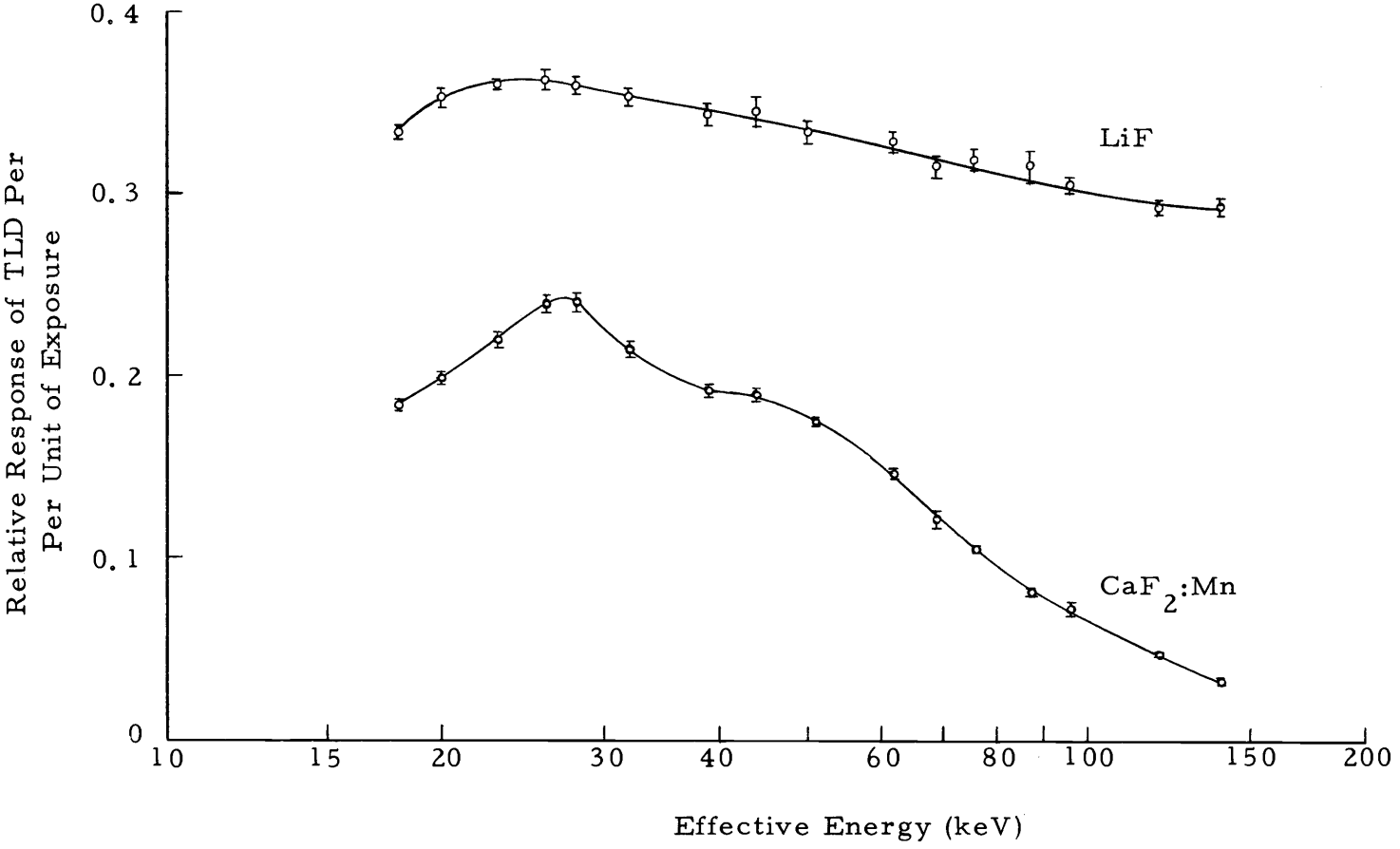

Figure 16. Relative response of lithium fluoride and calcium fluoride dosimeters vs. effective energy of x-ray beam.

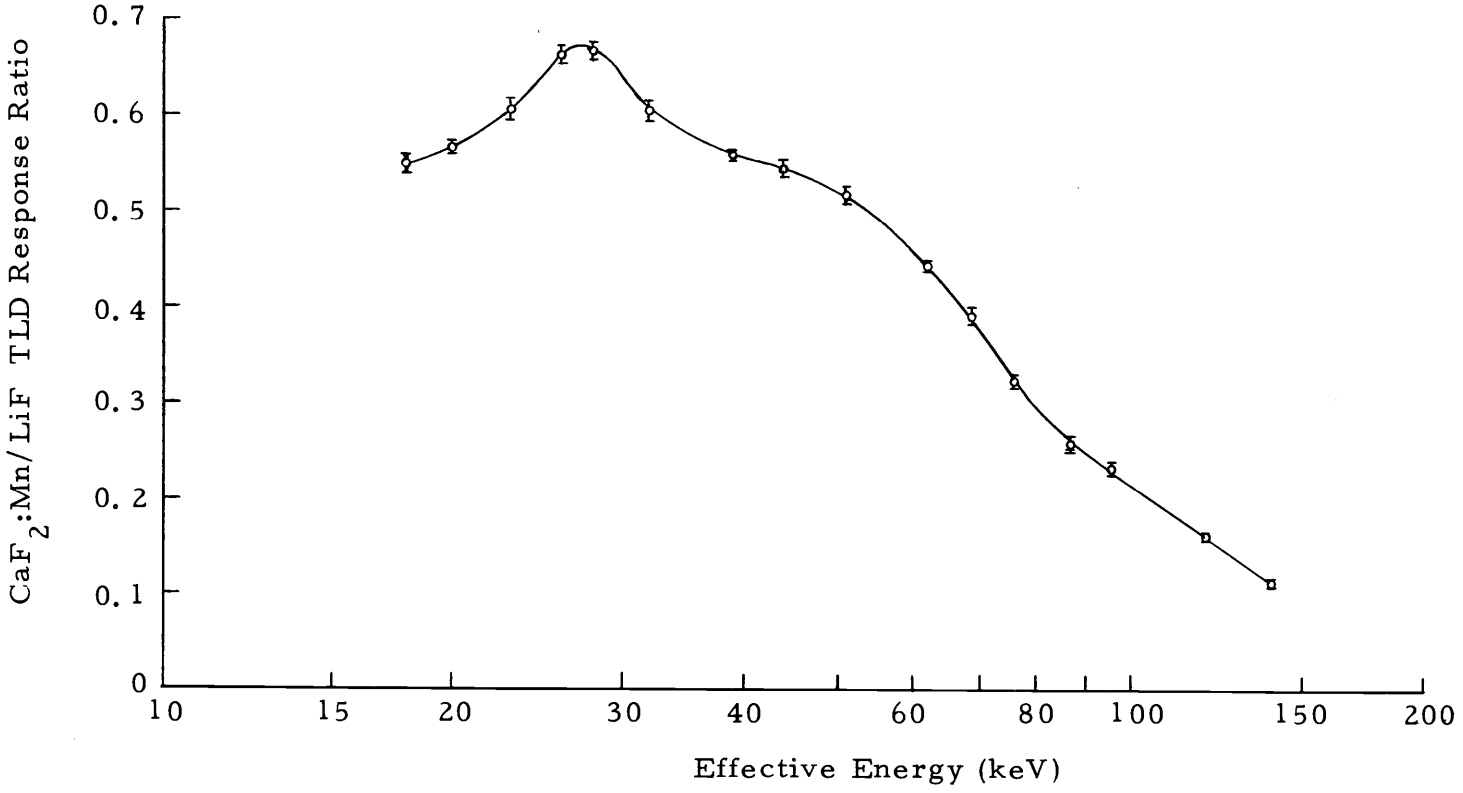

Figure 17. Ratio of calcium fluoride to lithium fluoride dosimeter response vs. effective energy of x-ray beam.

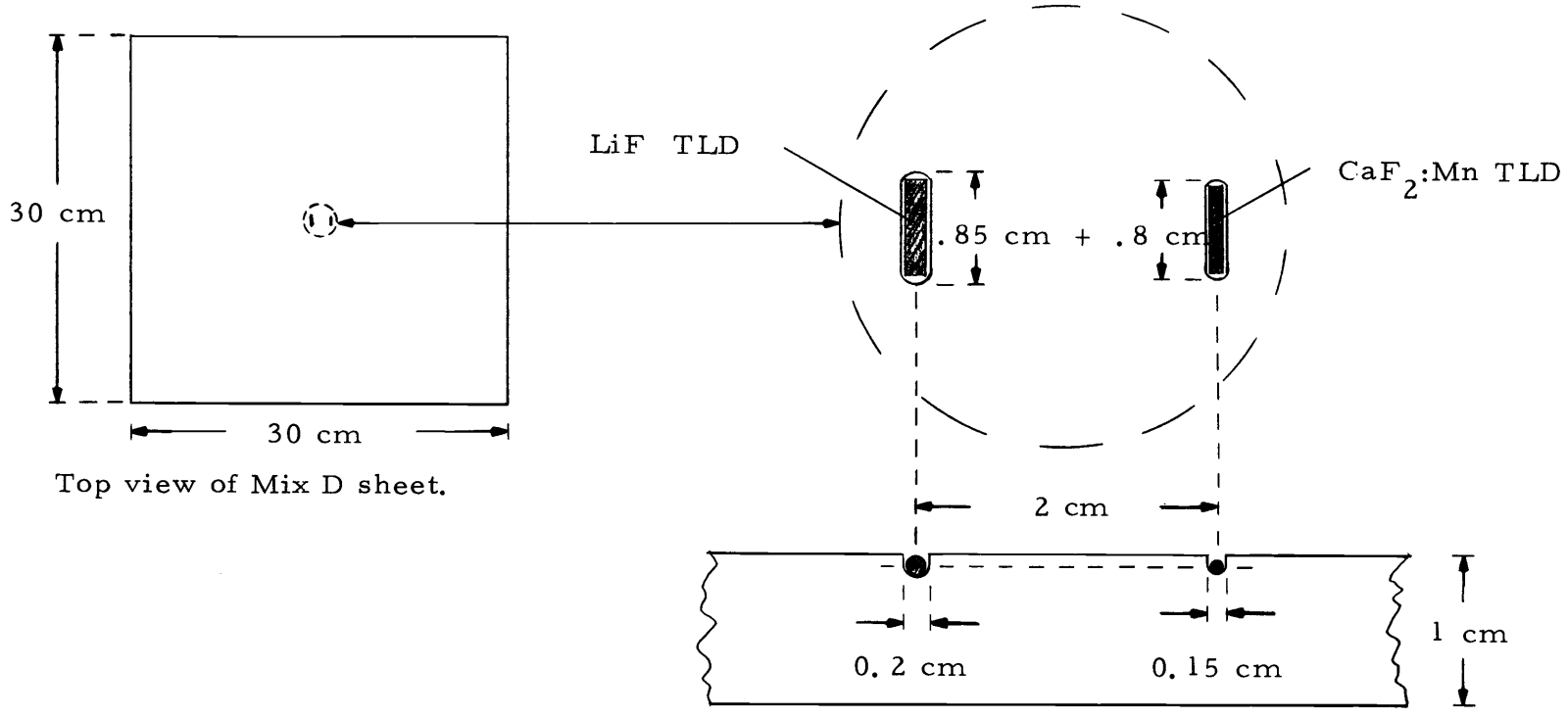

Figure 18. Dosimeter grooves carved in Mix D sheet.

15, and 25 cm with only a single pair of dosimeters placed in the phantom in each case. The results were normalized to a constant incident exposure. Similar measurements were then made with pairs of dosimeters placed at 1 cm intervals for depths from 0 to 13 cm, and at 2 cm intervals for depths from 15 to 25 cm, for a total loading of 20 dosimeter pairs.

The mean of the single-pair observations was compared to that for the twenty-pair observations, at each depth, using Student T tests at the 95 percent confidence level. Pooled estimates of the standard error of the means were used for this purpose. This procedure was replicated at 40, 100 and 150 kVp. The tests did not indicate that there were statisically significant differences in the measurements at any of the kVp-depth levels checked.

This result concurs with that of Hendee et al (38), who found that LiF capsules placed at one centimeter intervals in a phantom did not noticeably perturb the dose at any point along the central axis. Therefore, in all subsequent measurements, all twenty pairs of dosimeters were exposed in the phantom simultaneously.

Phantom Exposures

The phantom was placed on a standard radiographic table with a source-table distance of 40 inches; a distance often used for table-top radiography. Beam size at the table-top was 17 x 17 inches. The

dosimeters were arranged in the phantom as described above and were exposed at 40 kVp and 100 mA using the single-phase generator. The large dose range of the TLD allowed multiple exposures to be made to integrate sufficient dose for accurate readout of dosimeters at the greater depths, as well as for those placed in the upper portions of the phantom. Minimum and maximum exposure levels obtained were approximately 100 and 100,000 mR, respectively. After readout and annealing, the dosimeters were replaced in the same positions within the phantom and the exposure was repeated using the three-phase generator. KVp, mA, distance, and timer settings were the same as those used for the single-phase exposure. Two sets of measurements were made in this manner at 40, 60, 80 100, 125, and 150 kVp.

IV. RESULTS AND DISCUSSION

Effective X-Ray Beam Energy

The ratio of CaF_2:Mn to LiF dosimeter response was plotted as a function of depth within the phantom. The data appeared to fit straight lines with slopes equal or close to zero, indicating slight change in the effective energy of the x-ray beam as it passed through the phantom. Regression lines of response ratio on depth were fitted to the data for each combination of kilovoltage and power-phase. Figure 19 is an example of such a fit. Statistical F and T tests were used to test the hypotheses that the slopes of the individual lines were equal to zero. The hypotheses could not be rejected at the 95% confidence level, and it was decided to use the average response ratios for the energy determinations. The energy data were then used to read relative LiF response from Figure 16. From these, correction factors were determined for the LiF dosimeters and are shown in Table 5.

The fact that the effective energy of the x-ray beam may change only slightly within a tissue equivalent medium has been previously reported in the literature (17, 40, 77). The effective energy at depth is a function of the area of the phantom irradiated, the depth within the phantom, and the energy spectrum of the incident x-ray beam. The occurrence of two opposing effects leads to the small change in

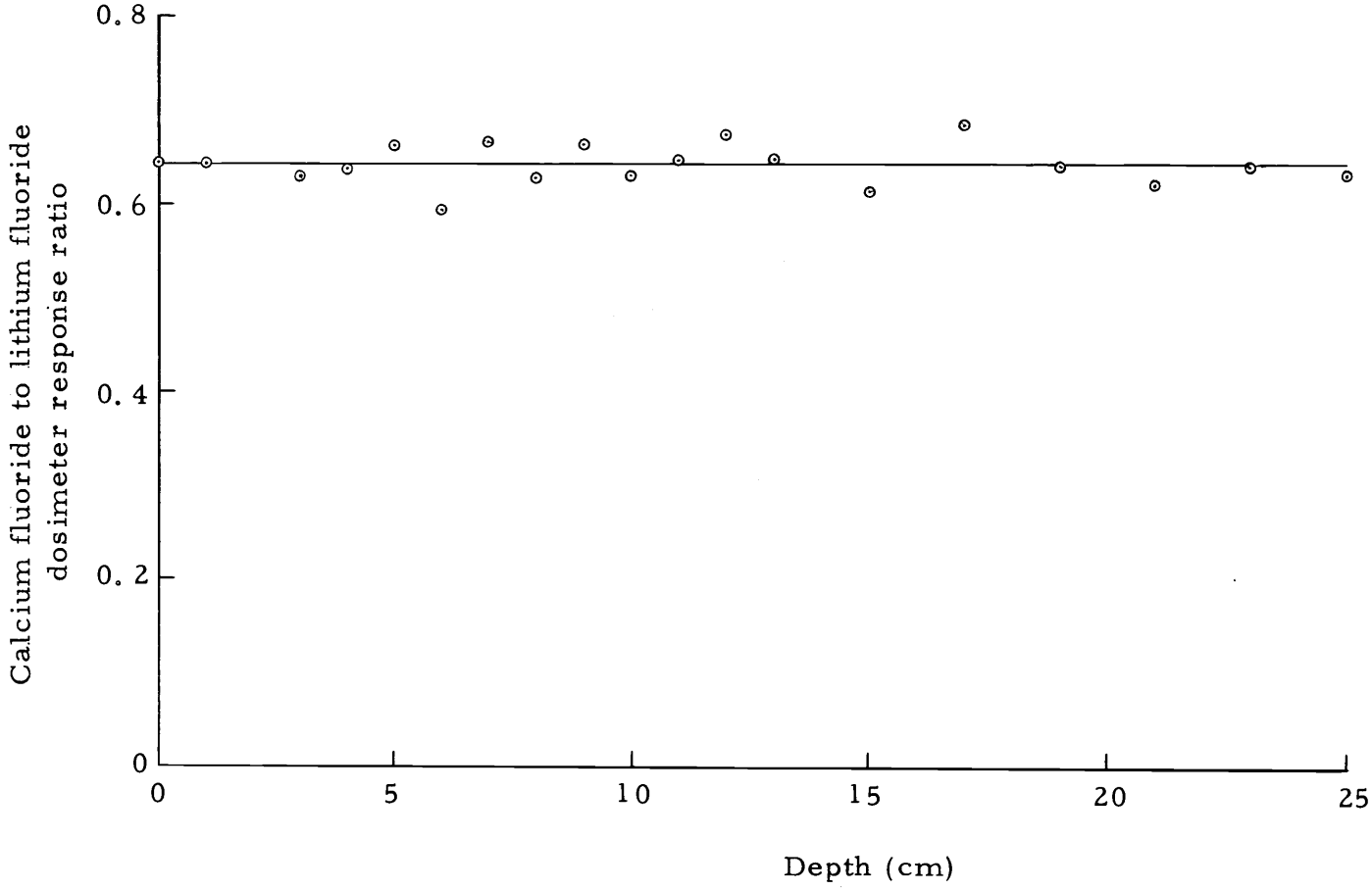

Figure 19. Ratio of calcium fluoride to lithium fluoride dosimeter response vs. depth in Mix D phantom for 125 kVp x rays.

Table 5. X-ray beam effective energy and LiF dosimeter correction factors listed as a function of the kVp and power-phase.

kVp-phase	Effective Energy (keV)	LiF Correction Factor
40 - 1	18.0	2.99
40 - 3	18.3	2.94
60 - 1	19.2	2.88
60 - 3	20.9	2.81
80 - 1	21.8	2.78
80 - 3	22.2	2.77
100 - 1	22.4	2.76
100 - 3	23.9	2.75
125 - 1	24.9	2.75
125 - 3	25.4	2.75
150 - 1	25.7	2.75
150 - 3	27.5	2.76

effective energy (30).

The primary beam increases in effective energy as the lower energy components are selectively filtered out. This effect is independent of beam area and quality (85). However, in a material of low atomic number, a major proportion of the x-ray interactions in the diagnostic energy region occur by Compton effect which produces scattered photons of lower energy than the primary photons. These scattered photons tend to compensate for the loss of the low-energy primary photons with the result that the effective energy of the x-ray beam along the central axis is almost unchanged.

At low incident photon energies, the contribution to the central axis from scatter is relatively small due to the short range of the low-energy scatter photons. Thus, there is a tendency toward a slight increase in effective energy with depth (17).

As the incident x-ray energy increases, the contribution from scattered radiation also increases (97). At beam energies in the upper range of, and above the diagnostic kilovoltage range, this effect tends to produce a decrease in effective energy with increasing phantom depth (30).

Depth Dose Measurements

In determining absorbed dose, it is often convenient to first measure the exposure, and from this, calculate the absorbed dose

(104). The following equation may be used for this purpose:

$$D_{med} = X f_{med}$$

where D_{med} is the absorbed dose at the point of interest in the medium, expressed in rads, X is the exposure at the point of interest in the medium, expressed in roentgens, and f_{med} is the roentgen to rad conversion factor (14). The value of f_{med} varies as a function of the x-ray beam energy. Mean values integrated over typical x-ray spectra are listed in ICRU report 10b (44).

The practice followed in this study has been to use exposure measurements in all graphs and calculations. When absorbed dose is specifically required, the exposure is multiplied by the appropriate factor. The conversion factor for tissue in the x-ray energy range involved here is a constant having a value of 0.923 (44).

Figures 20 through 25 show the relative single-and three-phase exposures vs. phantom depth. These measurements were made for a source to table-top distance of 40 inches. This data however, may be converted to other distances by means of formulae developed for this purpose (42, 46, 48, 61). Agreement with experimental data using these methods, has been reported to be within $\pm$ 2% (7) whereas conversion by merely applying inverse-square-law leads to greater error (50).

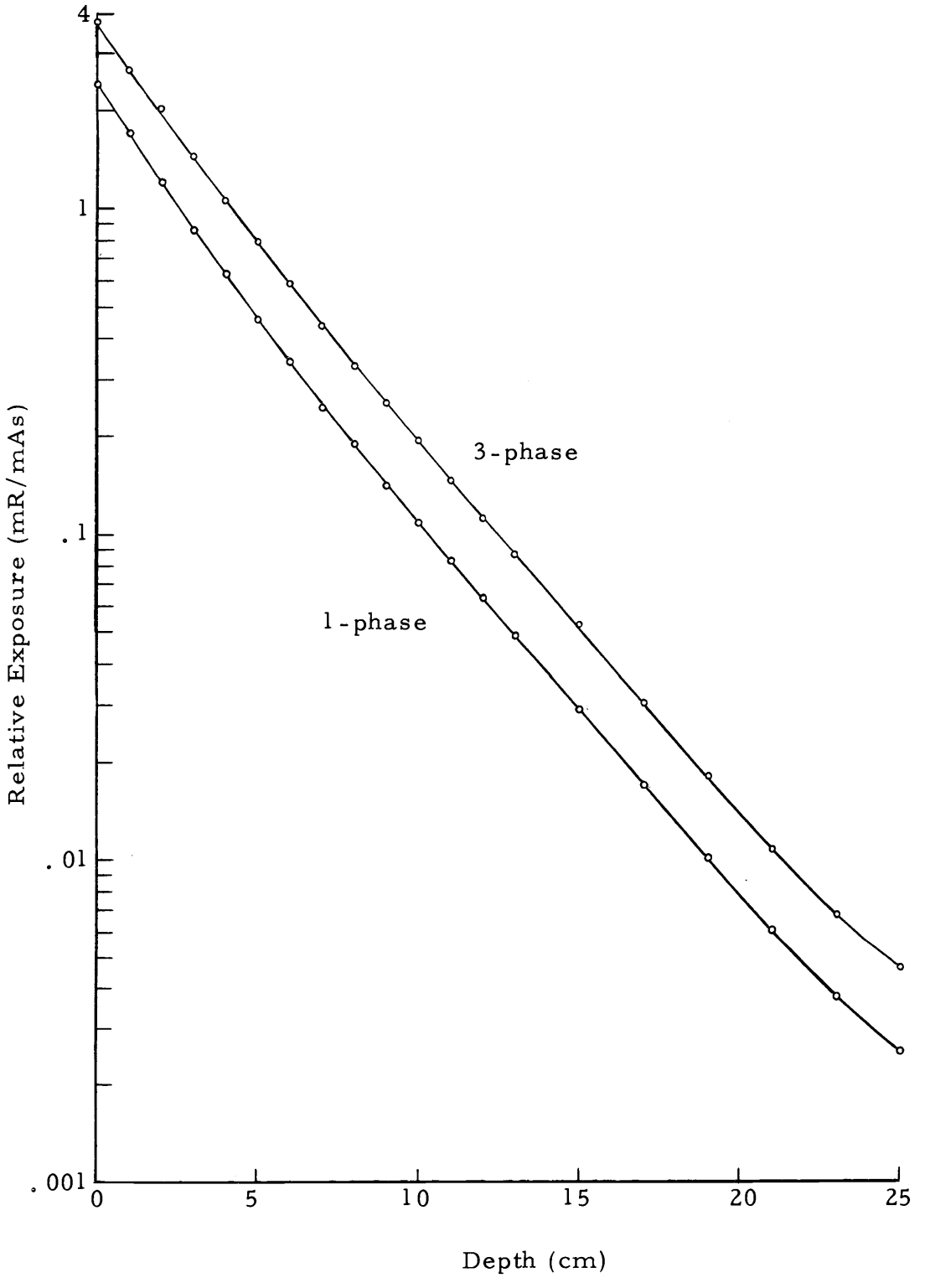

Figure 20. Relative exposure of 40 kVp x rays vs. depth in Mix D phantom.

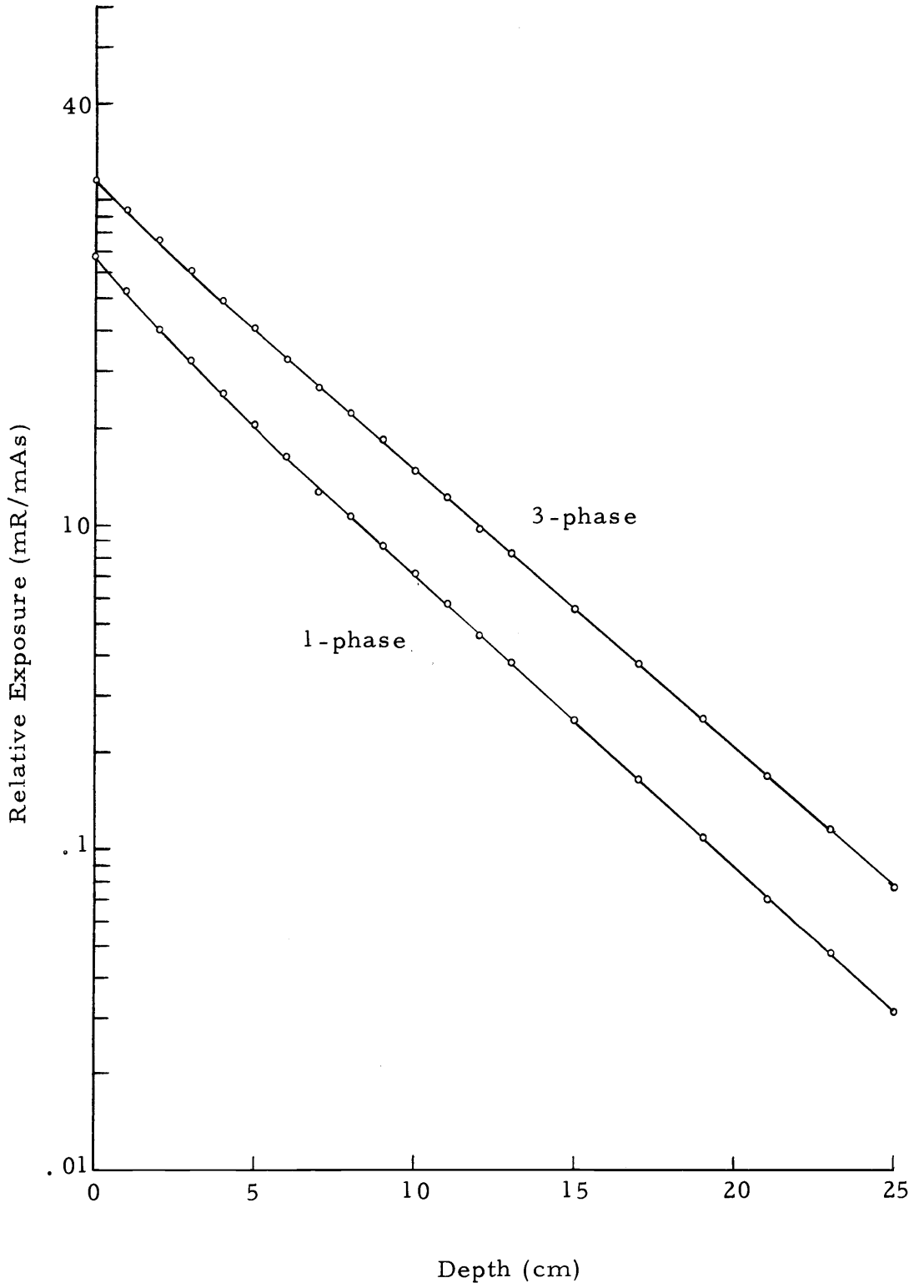

Figure 21. Relative exposure of 60 kVp x rays vs. depth in Mix D phantom.

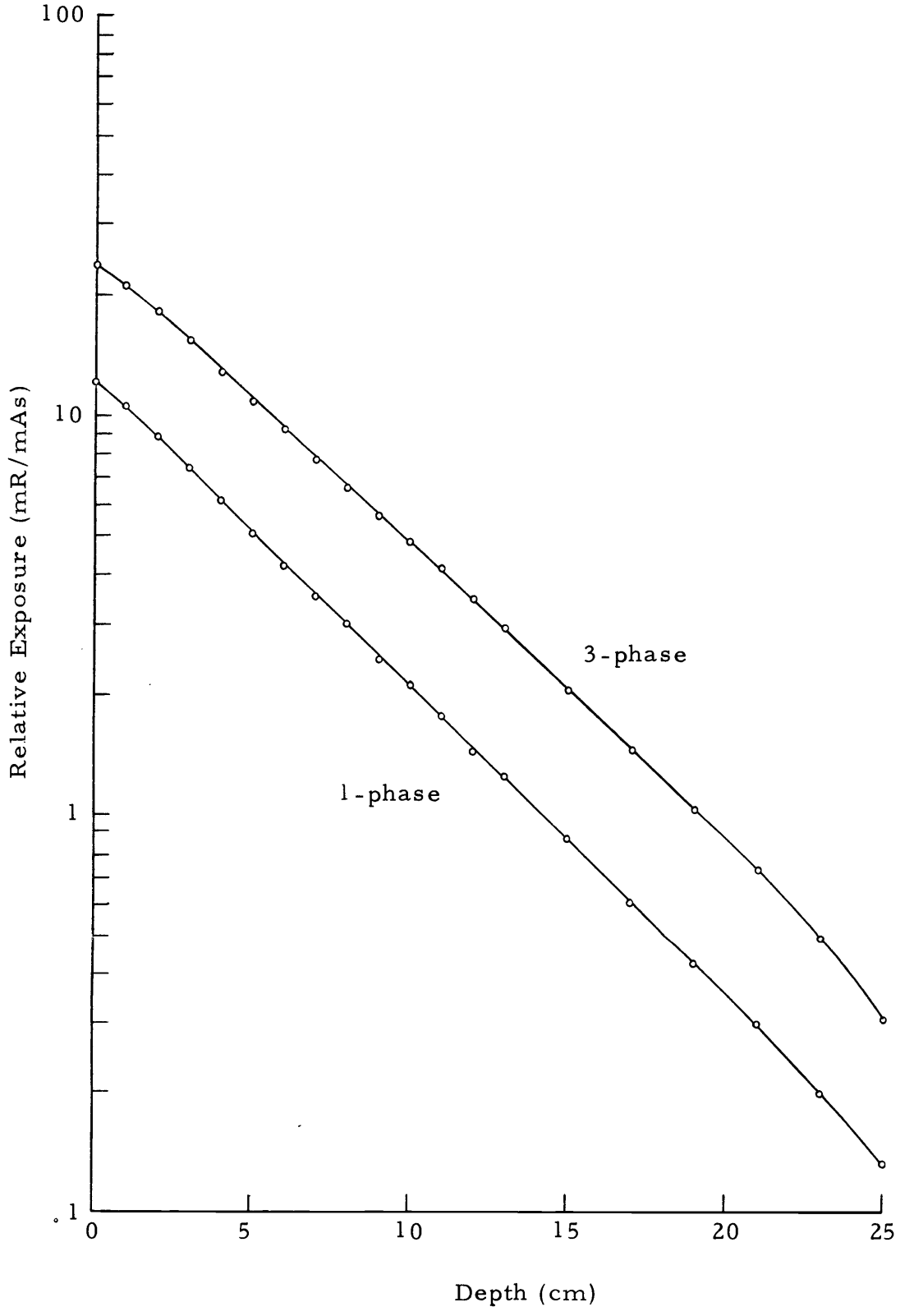

Figure 22. Relative exposure of 80 kVp x rays vs. depth in Mix D phantom.

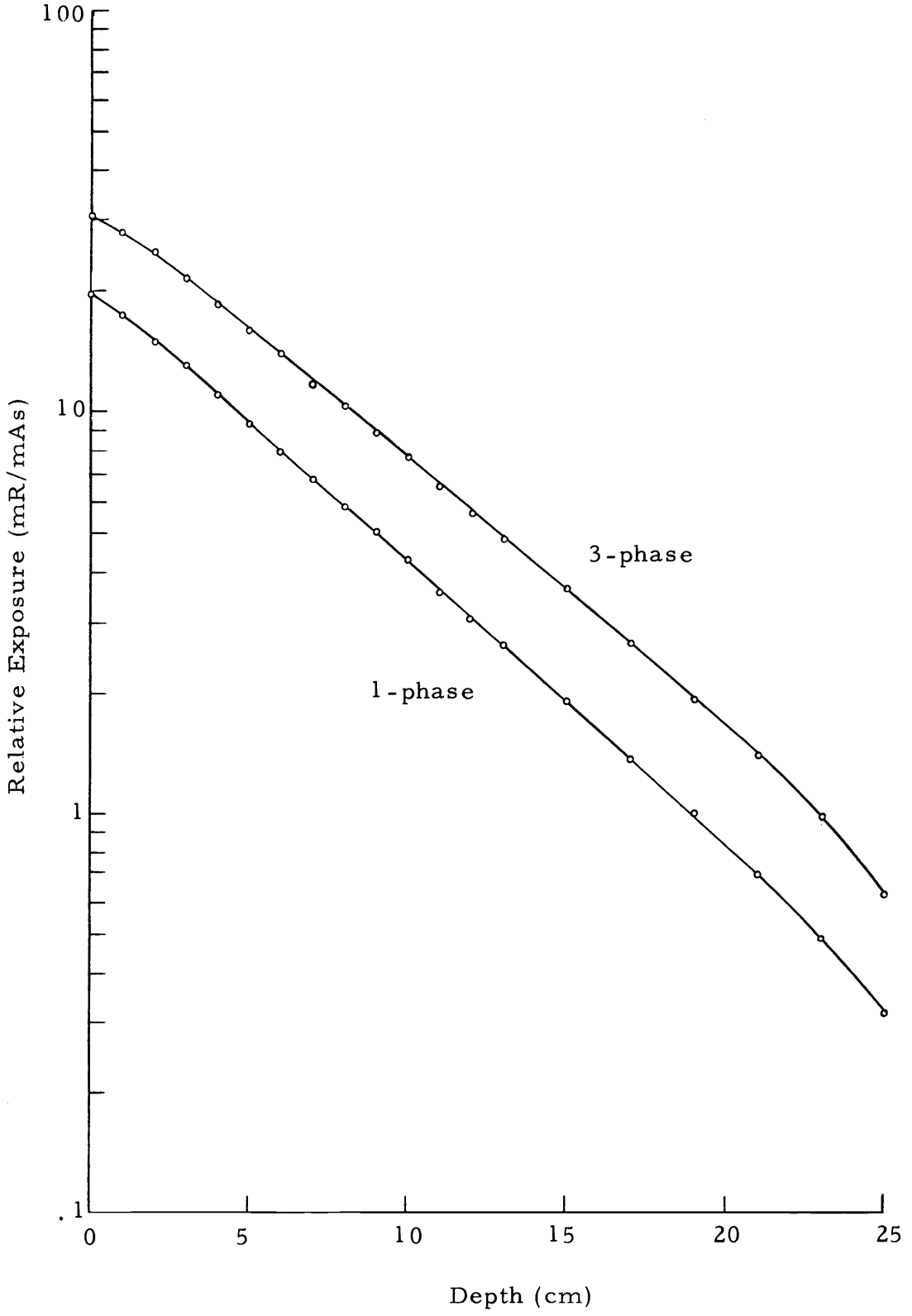

Figure 23. Relative exposure of 100 kVp x rays vs. depth in Mix D phantom.

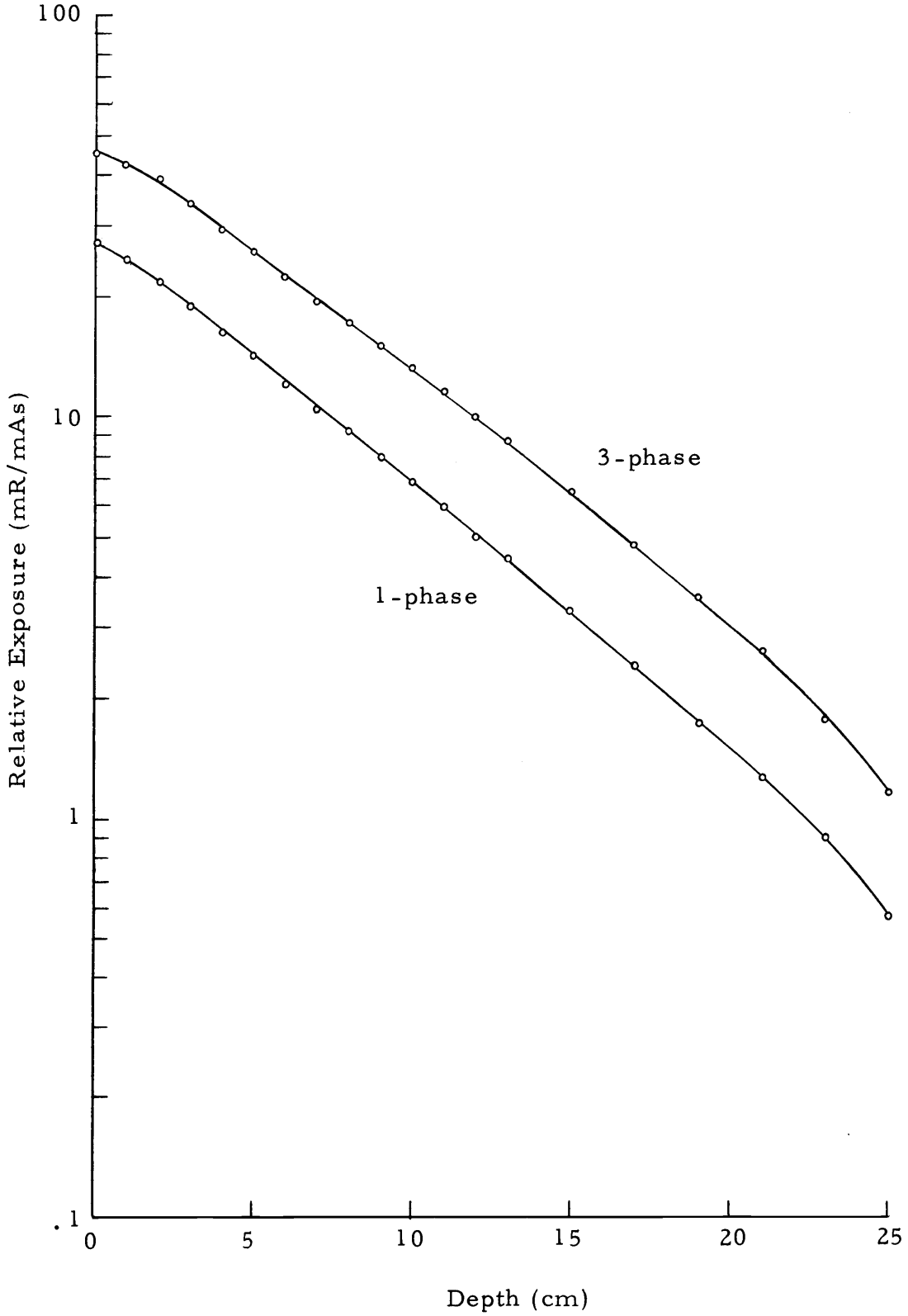

Figure 24. Relative exposure of 125 kVp x rays vs. depth in Mix D phantom.

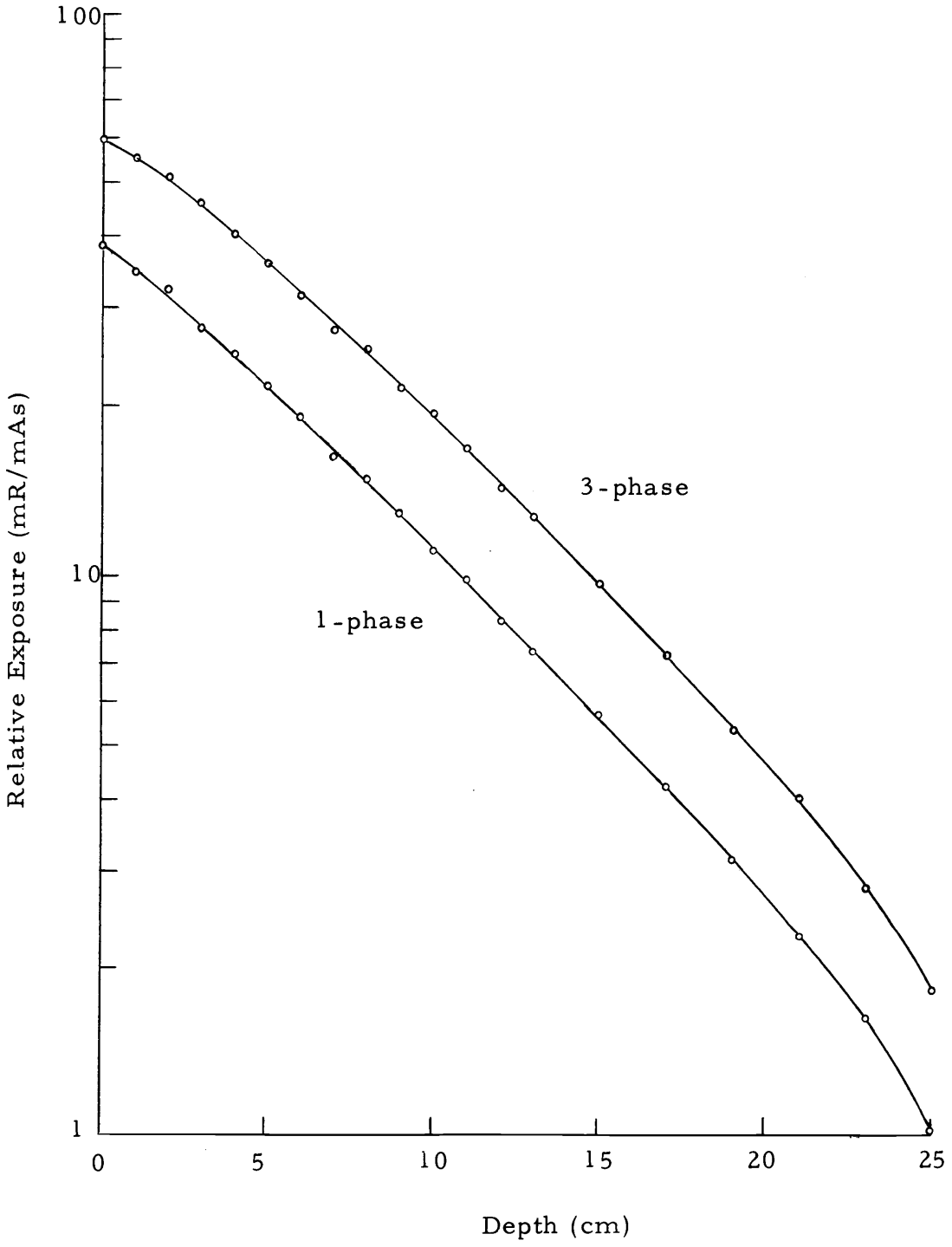

Figure 25. Relative exposure of 150 kVp x rays vs. depth in Mix D phantom.

X-Ray Beam Output

The surface exposures are an indication of the output differences between single- and three-phase x-ray generators operating at the same kilovoltage. Because of the difference in beam quality, the exposure differences become greater with increasing phantom depth.

Table 6 lists the ratio of three-phase to single-phase exposure per milliampere-second (mAs) as a function of kilovoltage and depth within the phantom. As seen from this Table, the increase in mAs required to achieve the same exposure within the phantom, for single-phase as for three-phase, varies from 1.55 to 2.40.

Dose Differential Using Equal Kilovoltages

A derivation was made of the dose increase resulting from the use of single-phase rather than three-phase x-ray equipment operating at the same kilovoltage. To do this, the single-phase curves were multiplied by normalizing factors which were chosen such that the single- and three-phase exposures would be equal at a specified depth within the phantom. The depths, which were chosen to be consistent with anatomical thicknesses typically radiographed at each particular kilovoltage, are shown in Table 7.

Table 6. Ratio of three-phase to single-phase exposure per milliampere-second as a function of kVp and Mix D phantom depth.

	Phantom Depth (cm of Mix D)				
	0	5	10	15	25
Kilovoltage	Exposure Ratio				
40	1.55	1.74	1.77	1.78	1.78
60	1.69	2.00	2.11	2.22	2.28
80	1.96	2.14	2.25	2.36	2.40
100	1.77	1.86	2.01	2.13	2.20
125	1.68	1.80	1.91	1.98	2.05
150	1.55	1.65	1.71	1.74	1.80

Table 7. Phantom depths at which single- and three-phase roentgen exposures were normalized to be equal.

Kilovoltage (kVp)	Phantom Depth (cm)
40	5
60	10
80	15
100	25
125	25
150	25

The difference in dose resulting from the use of single-phase equipment is shown plotted as a function of depth within the phantom in Figures 26 and 27. As can be seen from these graphs, dose differential, which is expressed as a percent of the three-phase dose, increases with increasing kilovoltage, reaching a peak at 100 kVp. It then decreases as the kVp continues to increase. In every case, the greatest percent difference in dose occurs at the phantom surface.

A possible explaination for this variance of dose differential with kilovoltage is that, at the lower kilovoltages, only the photons relatively close to the peak photon energy are able to contribute significantly to the dose. The lower energy photons are readily absorbed by the x-ray tube-housing filtration. Thus, the difference between the lower kilovoltage single- and three-phase x-ray beams, as they leave the

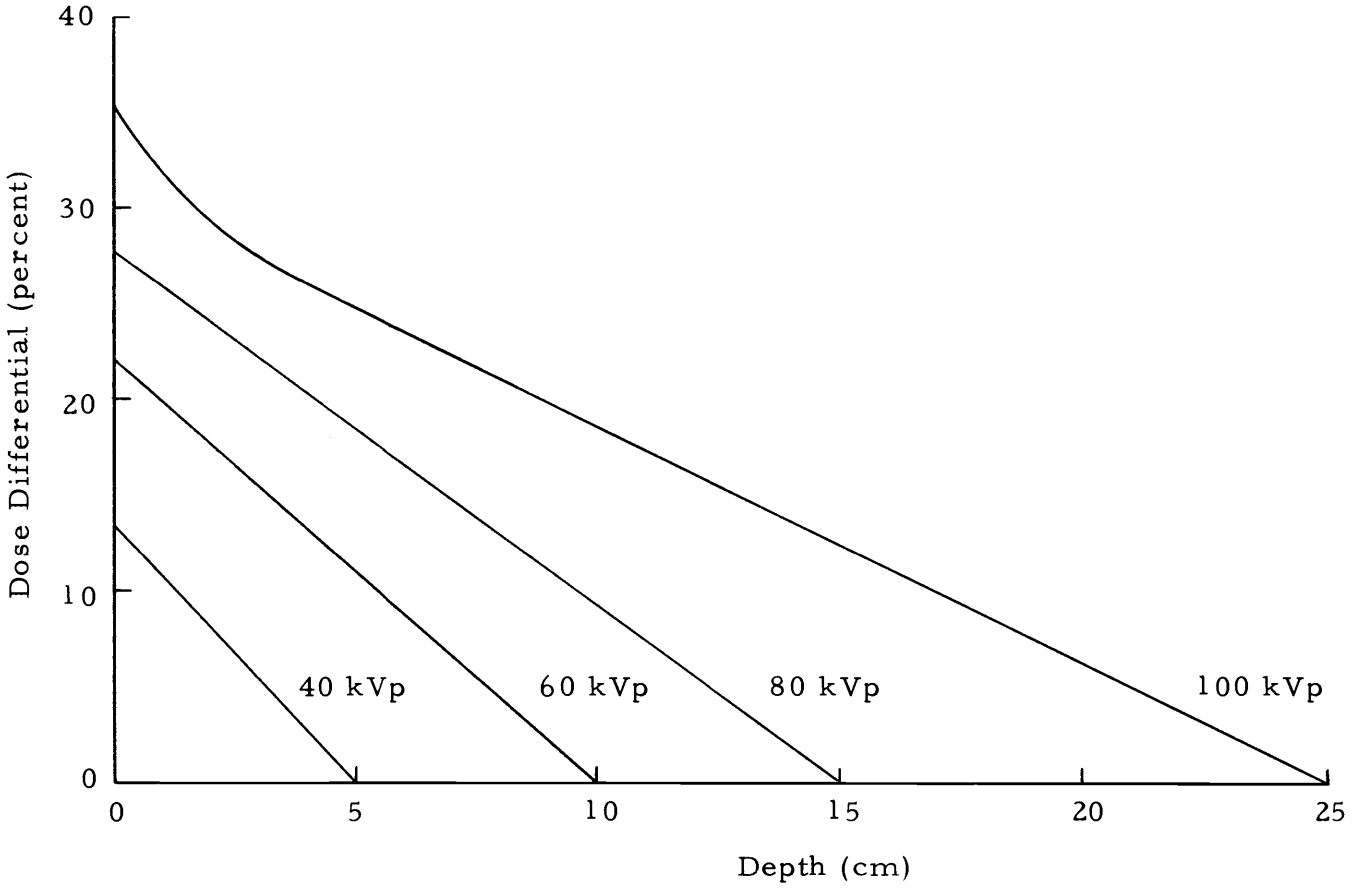

Figure 26. The difference between single- and three-phase depth-doses at 40, 60, 80 and 100 kVp. Data is normalized for equal exit exposures and dose differential is expressed as a percent of the three-phase dose.

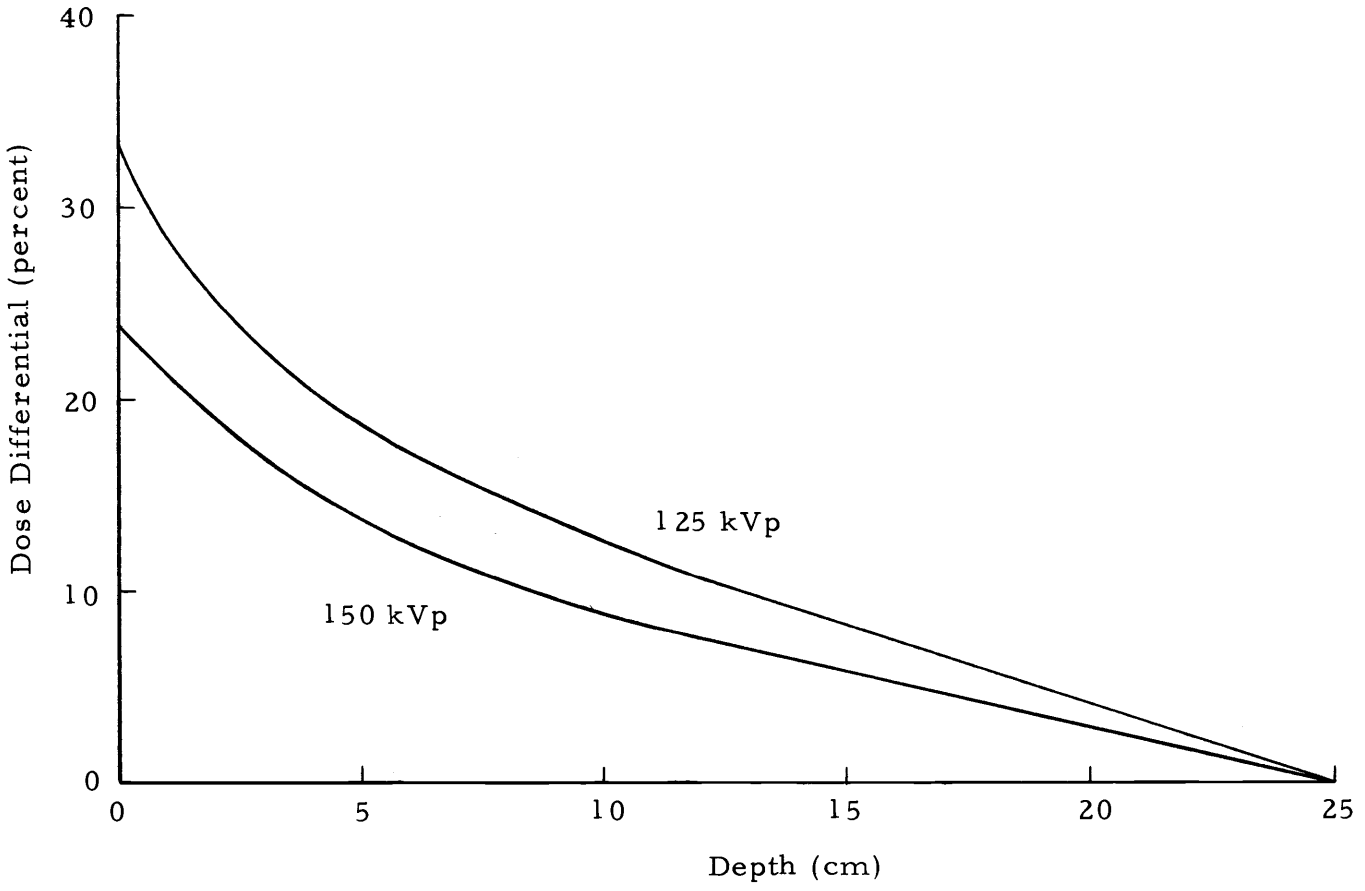

Figure 27. The difference between single- and three-phase depth-doses at 125 and 150 kVp. Data is normalized for equal exit exposures and dose differential is expressed as a percent of the three-phase dose.

tube-housing, is due primarily to a difference in the number of photons rather than in the energy of the photons.

As the kilovoltage increases, a greater proportion of the x rays produced by the lower energy electrons are able to penetrate the filtration and contribute to the dose in the phantom. The dose differential increases as the difference in the effective energy of the x-ray beams increases.

This effect, however, is eventually counteracted by scattered radiation. As indicated above, the proportion of the dose contributed by scattered radiation increases with increasing kilovoltage. Because high energy photons suffer a greater percentage change in energy in a given Compton scatter interaction than do lower energy photons,[19] the difference in the energy spectrum between single-phase and three-phase generated x rays scattered within a phantom is less than that of the primary beams.

Equivalent Kilovoltages

If a single-phase x-ray generator was actually being used interchangeably with a three-phase unit, the kilovoltage would probably be adjusted to provide, as nearly as possible, the same radiographic

---

[19] As an example of this, x-ray photons of energy 100 and 150 keV are considered in 90° Compton scatter interactions. The scatter photons from these events will be 116 and 84 keV, representing energy losses of 23 and 16 percent, respectively.

results.

For a given subject, screen-film combination, and source-subject-film geometry, the visibility of a detail in a radiograph is governed by degree of film darkening and subject contrast. Though these two aspects of a radiograph are not totally independent, they may, for practical purposes, be thought of as being related to x-ray beam quantity and quality, respectively.

It was previously shown that the quantity and quality differences between the single- and three-phase x-ray beams are due to differences in kilovoltage waveform. These two factors were each used as a criterion for determining equivalent single-phase and three-phase kilovoltages.

X-Ray Beam Quantity as Criterion

From Figures 20 through 25, curves of relative exposure (mR/mAs) vs. kilovoltage were derived for phantom depths of 5, 10, 15, and 25 cm, for both single- and three-phase x-ray units. They are shown in Figures 28 and 29. From these, equivalent kilovoltages were derived with the criterion that the relative exposure for single-phase be equal to that for the three-phase at each of the phantom depths measured. The results are shown in Table 8. Since the change in single-phase kilovoltage, as a function of phantom depth, is considered too small to be of practical significance, the data were averaged

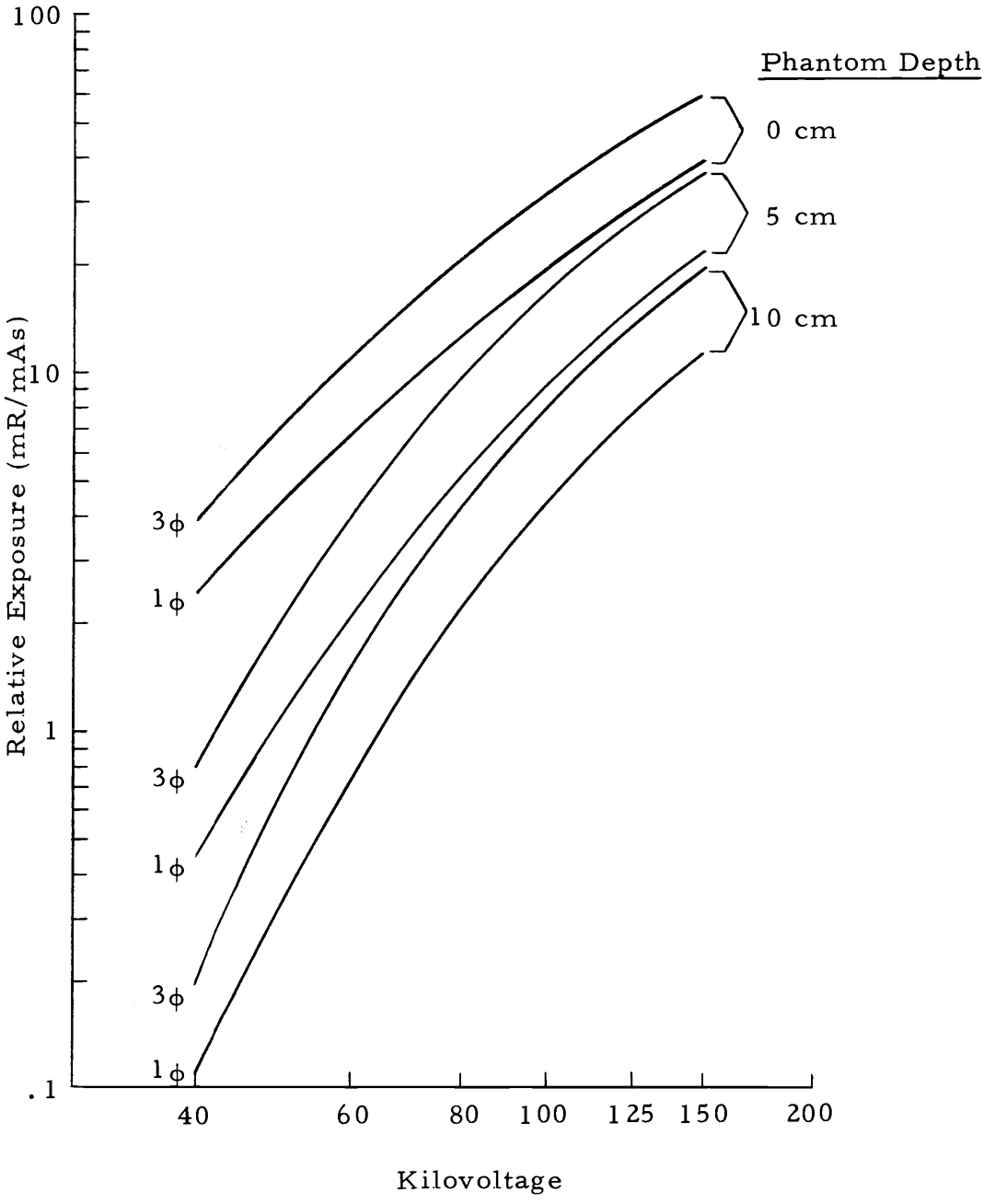

Figure 28. Relative exposure vs. kilovoltage for phantom depths of 0, 5, and 10 cm.

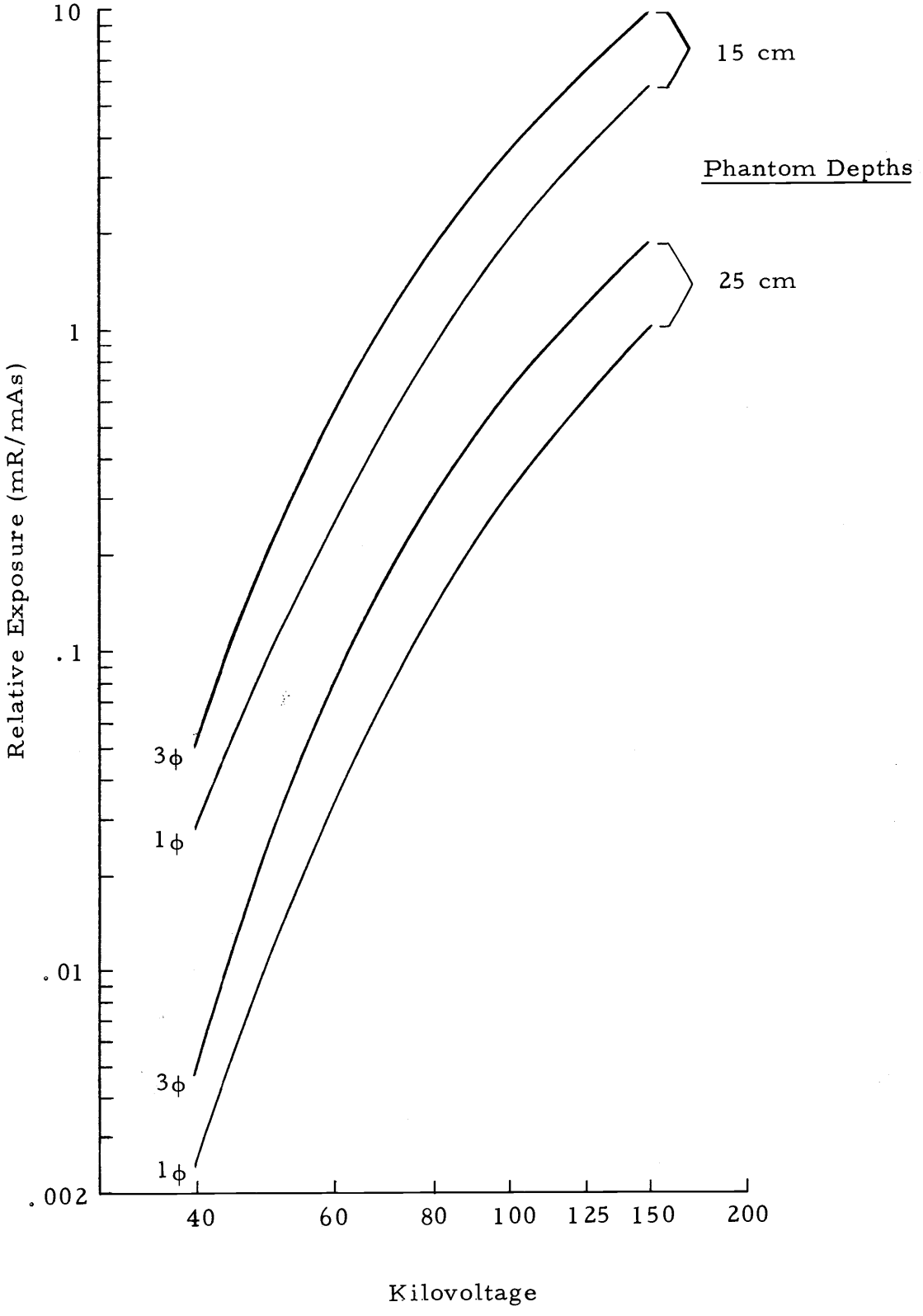

Figure 29. Relative exposure vs. kilovoltage for phantom depths of 15 and 25 cm.

Table 9. Equivalent kilovoltages based upon equal single- and three-phase relative exposures (mR/mAs) at phantom depths shown.

Three-Phase Kilovoltage	Phantom Depth (cm of Mix D)				
	5	10	15	25	Average
	Single-Phase Kilovoltage				
40	46	46	44	44	45
50	59	59	58	58	58
60	73	73	72	72	72
70	87	86	85	85	86
80	102	99	98	98	99
100	130	128	127	127	128
120	-	-	150	150	150

over all depths and are shown plotted in Figure 30.

X-Ray Beam Quality as Criterion

Figures 20 through 25 were used to calculate percent depth exposure, that is, the relative depth exposure expressed as a percent of the surface exposure. This factor is obviously determined by the penetrating ability of the x-ray beam, i. e. its quality. The percent depth exposure for each combination of kilovoltage and power-phase are shown plotted in Figure 31. From these, percent depth exposure vs. kilovoltage curves were derived for phantom depths of 5, 10, 15, and 25 cm, for both single-phase and three-phase units. They are shown in Figure 32. Equivalent kilovoltages were then derived with the criterion that the percent depth exposure for single-phase be equal to that for three-phase at each phantom depth measured. The results are shown in Table 9. As before, the change in single-phase kilovoltage as a function of phantom depth is not considered to be of practical significance and the data were averaged over all depths. They are shown plotted in Figure 30.

Dose Differential Using Equivalent Kilovoltages

Three phantom depth exposure comparisons were made using equivalent kilovoltages. Values which had given the greater percent dose differentials when using equal single-phase and three-phase kVp

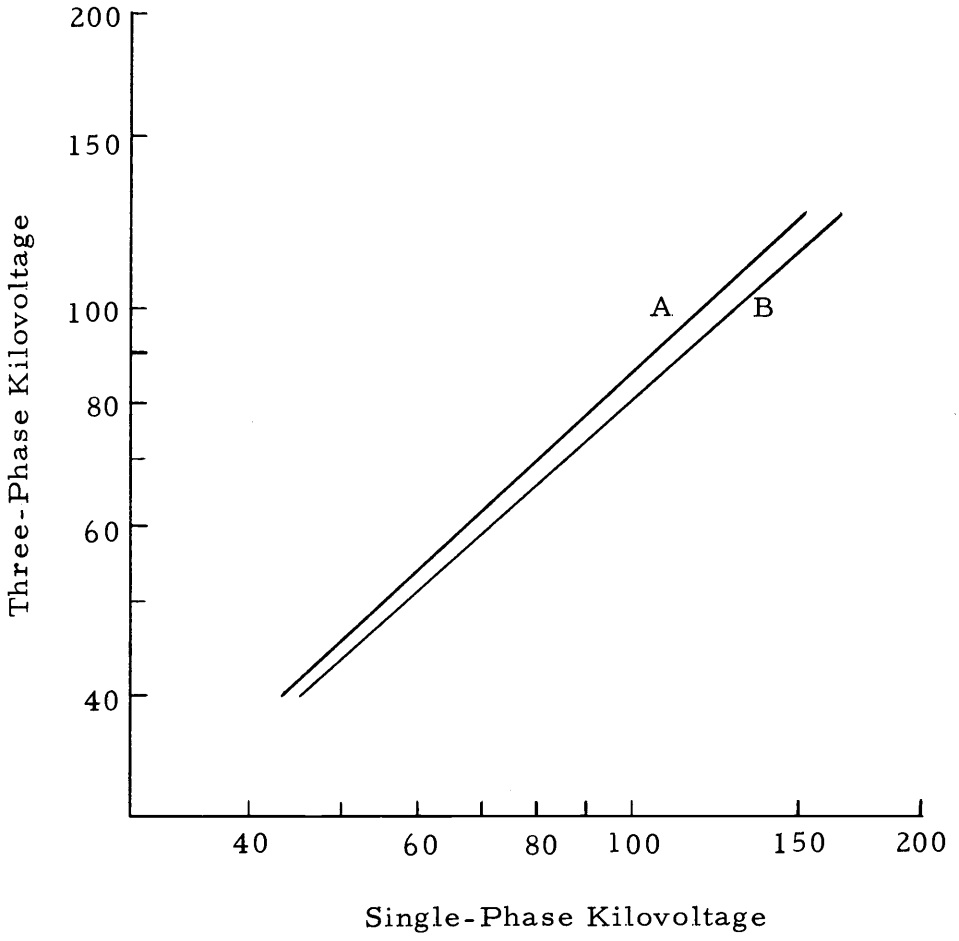

Figure 30. Equivalent kilovoltages for single-phase and three-phase x-ray systems.

Curve A is based upon percent depth exposure. Curve B is based upon relative depth exposure.

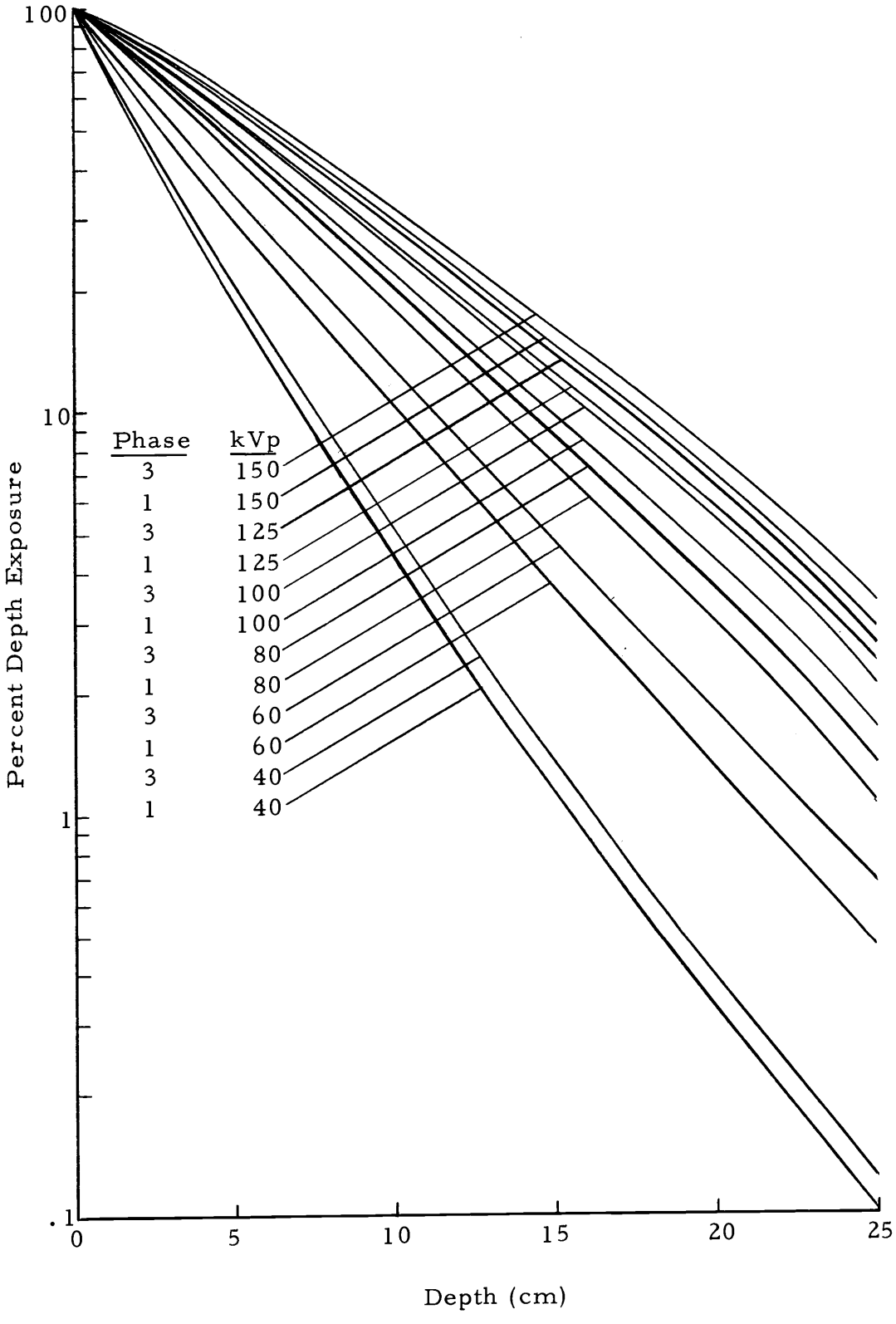

Figure 31. Percent depth exposure vs. depth in Mix D phantom.

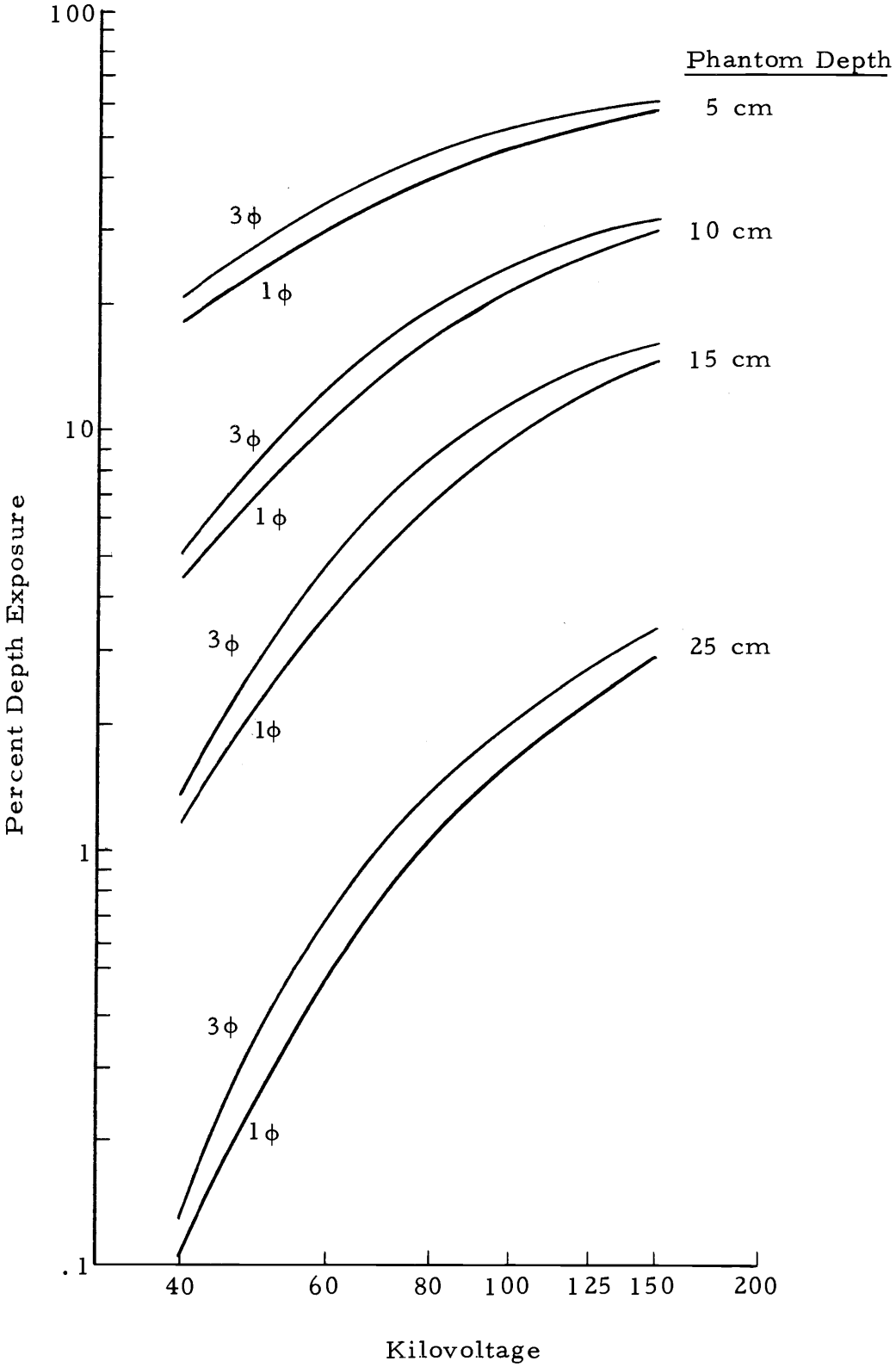

Figure 32. Percent depth exposure vs. kilovoltage.

Table 9. Equivalent kilovoltages based upon equal single- and three-phase percent depth exposure* at phantom depths shown.

Three-Phase Kilovoltage	Phantom Depth (cm of Mix D)				
	5	10	15	25	Average
	Single-Phase Kilovoltage				
40	44	42	42	42	43
50	58	54	54	56	56
60	69	67	67	67	68
70	82	79	80	79	80
80	95	92	93	91	93
100	122	118	118	115	118
125	150	147	147	143	147

*Percent depth exposure is the relative depth exposure expressed as a percent of the surface exposure.

were selected for the three-phase kilovoltages in this trial: 60, 80, and 100 kVp. Equivalent single-phase kilovoltages, which were taken from the percent depth dose curve in Figure 30, were 68, 93, and 118 kVp, respectively.

The three-phase depth exposure curves for 60, 80, and 100 kVp are shown in Figure 33. The data points shown are for single-phase measurements made at equivalent kilovoltages. Adjustments equivalent to approximately a 12% increase in mAs have been made to normalize the single-phase exposure to be equal to the 60, 80, and 100 kVp three-phase exposures at phantom thicknesses of 10, 15, and 25 cm, respectively. This is the same procedure used previously to derive dose differential. As can be seen from Figure 33, there was negligible difference in dose when equivalent kilovoltages were used.

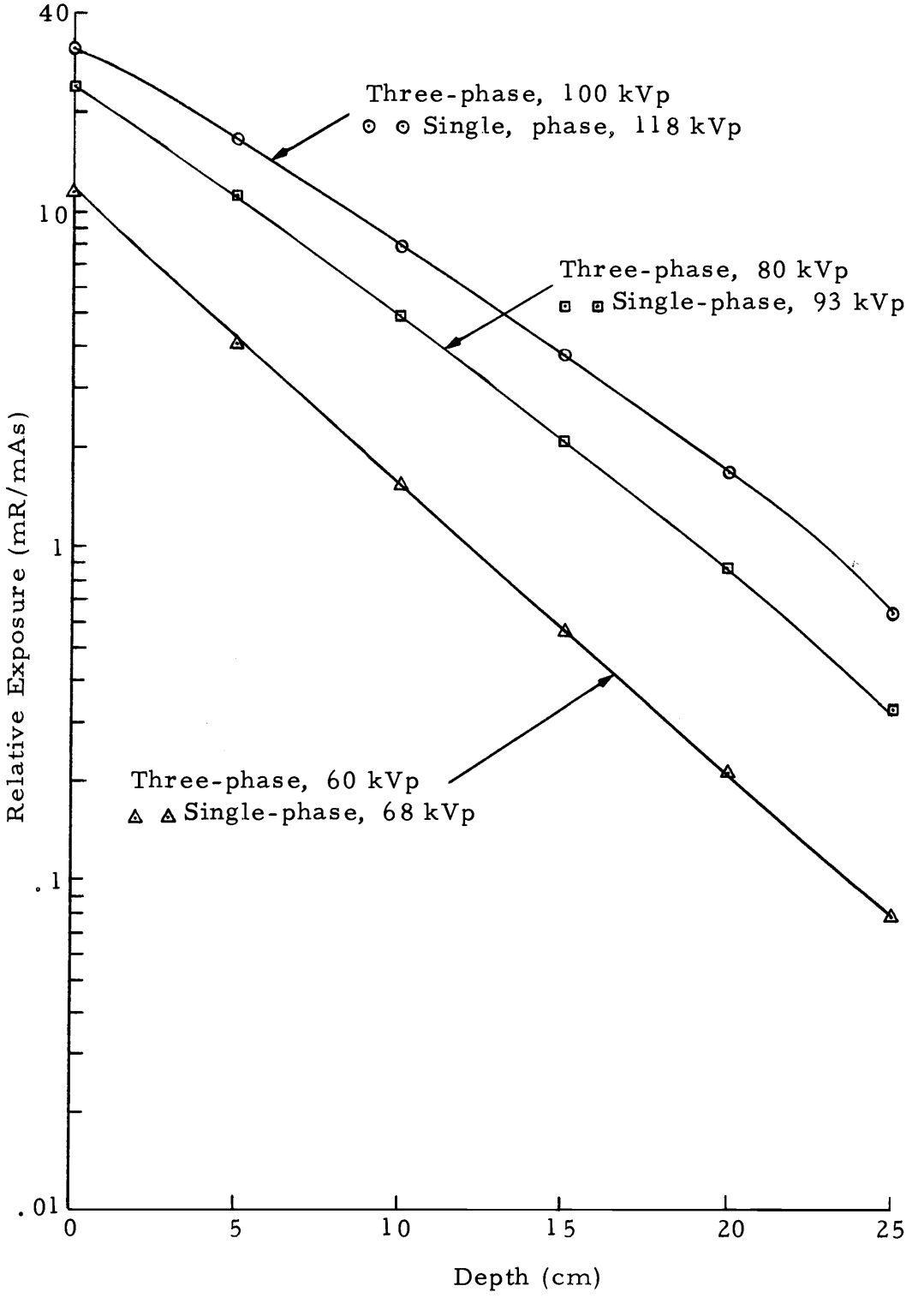

Figure 33. Three-phase depth exposure curves with equivalent kilovoltage single-phase data points superimposed.

V. CONCLUSIONS

The information derived from this study leads to the following conclusions:

(1) Three-phase diagnostic x-ray systems, having kilovoltage waveforms with less ripple, produce x-ray beams of higher effective energy than do single-phase systems operating at the same peak kilovoltage.

(2) When single-phase and three-phase systems are used to perform a given radiographic examination, the kilovoltages can be adjusted to provide equivalent x-ray beam quality to produce similar radiographic results. There is no appreciable difference in the dose distributions when this is done.

If equal tube currents are used under these conditions, the exposure time required by three-phase systems will be 80 to 90 percent of that required by single-phase.

(3) When single-phase and three-phase systems are operated at equal peak kilovoltages to perform a given radiographic examination, there is a divergence in the dose distributions, with the dose at a given depth being greater for single-phase systems. The dose differential is greatest at the incident surface, decreasing to zero at the exit surface.

(4) Single- and three-phase systems operated at equal peak kilovoltages do not produce radiographs of the same quality. The higher effective energy of the x-ray beam produced by the three-phase system results in lower contrast with less visibility of detail.

(5) When equal kilovoltages and tube currents are used, three-phase systems can produce radiographic exposures in 40 to 60 percent of the time required by single-phase systems.

(6) The higher tube-currents and greater tube-loading characteristics of three-phase systems make possible the very short exposure times required for certain radiographic procedures.

BIBLIOGRAPHY

1. Adams, G. D. On the use of thimble chambers in phantoms. Radiology 78:77-90. 1962.

2. Atlee, Z. J. and J. T. Perry. X-Ray generators. Bellwood, Illinois. Dunlee Corporation. n. d. 12 p.

3. Atlee, Z. J. and E. D. Trout. A study of roentgen-ray distribution at 60-140 kVp. Radiology 40:375-385. April, 1943.

4. Becker, K. Photographic, glass or thermoluminescence dosimetry? Health Physics 12:955-964. 1966.

5. Botden, P. J. M. Modern trends in diagnostic radiologic instrumentation. In: The reduction of patient dose by diagnostic radiologic instrumentation, ed. by R. D. Moseley and J. A. Rust. Springfield, Ill., Charles C. Thomas, 1964. p. 15-33.

6. Braestrup, C. B. Depth dose measurements for 100, 120, and 135 kv roentgen rays. Radiology 42:258-272. 1944.

7. Burns, J. E. Conversion of depth doses from one FSD to another. British Journal of Radiology 31:643. 1958.

8. Cameron, J. R., N. Suntharalingam and G. N. Kenney. Thermoluminescent dosimetry. Madison, Wisconson, University of Wisconson, 1968. 232 p.

9. Cameron, J. R., D. Zimmerman and G. Kenney. Thermoluminescent radiation dosimetry with lithium fluoride. Radiation Research 19:190. 1964.

10. Cameron, J. R. et al. Radiation dosimeter utilizing the thermoluminescence of lithium fluoride. Science 134:333-334. 1961.

11. Cameron, J. R. et al. Thermoluminescent radiation dosimetry utilizing LiF. Health Physics 10:25-29. 1964.

12. Carlsson, C. Integral absorbed dose from exposure measurements. Acta Radiologica Therapy Physics Biology. 1:443-458. 1963.

13. Compton, A. H. and S. K. Allison. X-rays in theory and experiment. 2d ed. Princeton, N. J., D. Van Nostrand, 1963. 838 p.

14. Cunningham, J. R. and H. E. Johns. The calculation of absorbed dose from exposure measurements: practical problem in dosimetry. Physics in Medicine and Biology 15:71-77. 1970.

15. Cusimano, J. P. and F. V. Cipperley. Personnel dosimetry using thermoluminescent dosimeters. Health Physics 14:339-344. 1968.

16. Ehrlich, M. Thermoluminescence response of LiF to x- and γ-rays: a study of rate and energy dependence over a wide range of exposures. Health Physics 12:1773. 1966.

17. Epp, E. R. and H. Weiss. Spectral fluence of scattered radiation in a water medium irradiated with diagnostic x-rays. Radiation Reserach 30:129-139. 1967.

18. Evans, R. D. The atomic nucleus. New York, McGraw-Hill, 1955. 972 p.

19. Facey, R. A. Dose and photon energy measurements for bone marrow in a human phantom by thermoluminescence. Health Physics 14:557-568. 1968.

20. Fowler, J. F. Solid-state dosimeters for in-vivo measurements. Nucleonics 21(10)·60-64. 1963.

21. Fowler, J. F. and E. Shuttleworth. Fading in thermoluminescent lithium fluoride used for radiation dosimetry. Nature 207:997-998. 1965.

22. Gager, R. M. Three-phase and three-phase relationships. Dunlee Digest 14:(1)1-2. 1969.

23. Gager, R. M. Three-phase radiography, pro and con. Dunlee Digest 7:(2)3. 1963.

24. General Electric Co. Rapid sequence ratings for General Electric rotating anode tube HDN-directive 13439. Milwaukee, Wis., 1968. 1 p.

25. Ginther, R. J. and R. D. Kirk. The thermoluminescence of CaF_2:Mn. Journal of the Electrochemical Society 104:365-369. 1957.

26. Glasser, O. et al. Physical foundations of radiology. 2d. ed. New York, Paul B. Hoeber, Inc. 1952. 581 p.

27. Goldstein, N., E. Tochilin and W. G. Miller. Millirad and megarad dosimetry with LiF. Health Physics 14:159-162. 1968.

28. Gorbics, S. G. and F. H. Attix. LiF and Ca_2F:Mn thermoluminescent dosimeters in tandem. International Journal of Applied Radiation 19:81-89. 1968.

29. Gorbics, S. G., F. H. Attix and J. A. Pfaff. Temperature stability of CaF_2:Mn and LiF (TLD-100) thermoluminescent dosimeters. International Journal of Applied Radiation and Isotopes 18:625-630. 1967.

30. Greening, J. R. and C. W. Wilson. The wavelength of the x radiation at a depth in water irradiated by beams of x rays. British Journal of Radiology 24:605-612. 1951.

31. Grigg, E. R. N. The trail of the invisible light. Springfield, Ill., Charles C. Thomas, 1965. 974 p.

32. Grodstein, G. W. X-ray attenuation coefficients from 10 keV to 100 MeV. Washington, D. C. 1957. 54 p. (U. S. National Bureau of Standards Circular 583).

33. Gustafson, R. B. Rectifiers and single- and three-phase comparison. In: High-tension generation and its use in radiography, ed. by W. L. Bloom, Jr., Milwaukee, Wis., General Electric Co., 1962. p. 32-41.

34. Gustafson, R. B. X-ray generation, single-phase, three-phase. Diagnostic Technical Letter No. 109, X-Ray Department, General Electric Co., July 10, 1962. 22 p.

35. Hale, J. and D. L. George. Physical factors in cinefluorography. American Journal of Roentgenology, Radium Therapy, and Nuclear Medicine 92:1189-1191. 1964.

36. Hall, R. M. and J. P. LaRocca. Thermoluminescent dosimeters for environmental monitoring. Health Physics 12:851-852. 1966.

37. Harris, A. M. and J. H. Jackson. Pre-irradiation annealing of TLD lithium fluoride. Health Physics 15:457-461. 1968.

38. Hendee, W. R. et al. Depth dose measurements with lithium fluoride. American Journal of Roentgenology, Radium Therapy and Nuclear Medicine 102:694-696. 1968.

39. Hendee, W. R. et al. LiF depth-dose measurements. Radiology 90:371. 1968.

40. Hettinger, G. and K. Liden. Scattered radiation in a water phantom irradiated by roentgen photons between 50 and 250 keV. Acta Radiologica 53:73-92. 1960.

41. Hynes, D. M. Assessment of a technique for coronary arteriography using 70 mm film. British Journal of Radiology 42:736-743. 1969.

42. Hospital Physicists' Association. Depth dose tables for use in radiotherapy. British Journal of Radiology. Supplement No. 10. 1961.

43. International Commission on Radiological Units and Measurements. Clinical dosimetry. Report 10d of the International Commission on Radiological Units and Measurements. Washington, D. C. 1963. 61 p. (U. S. National Bureau of Standards Handbook 87).

44. International Commission on Radiological Units and Measurements. Physical aspects of irradiation. Washington, D. C. 1964. 106 p. (U. S. National Bureau of Standards Handbook 85.)

45. Jackson, W. Dose assessment in diagnostic radiology. British Journal of Radiology 40:301-308. 1967.

46. Jackson, W. Formula for the effect on roentgen ray depth dose of a change in focal distance. Acta Radiologica Therapy Physics Biology 8:279-293. 1969.

47. Jennings, W. A. Roentgen radiation from a beryllium window tube. Acta Radiologica 33:435-484. 1950.

48. Johns, H. E., W. R. Bruce and W. B. Reid. The dependence of depth dose on focal skin distance. British Journal of Radiology 31:254-260. 1958.

49. Johns, H. E. and J. R. Cunningham. The physics of radiology. 3d. ed. Springfield, Ill., Charles C. Thomas, 1969. 800 p.

50. Johns, H. E., E. R. Epp and S. O. Fedoruk. Depth dose data 75 kVp to 140 kVp. British Journal of Radiology 26:32-37. 1953.

51. Jones, D. E. A. and H. C. Raine. Letter to editor. British Journal of Radiology 22:549-555. 1949.

52. Kanamori, H. Advantages of three-phase roentgen units. Acta Radiologica Diagnosis 6:91-96. 1967.

53. Kanamori, H. Effects of roentgen tube voltage and current waveforms in radiography. Acta Radiologica Therapy Physics Biology 4:68-80. 1966.

54. Karzmark, G. J., J. White and J. F. Fowler. Lithium fluoride thermoluminescence dosimetry. Physics in Medicine and Biology 9:273-285. 1964.

55. Kenney, G. N. and J. R. Cameron. X-ray beam quality measurements utilizing TL dosimeters. U. S. AEC Division of Technical Information. 1963. (Progress Report, AEC Contract No. AT(11-1)-1105. 26 p.)

56. Liden, K. Errors introduced by finite size of ion chambers in depth dose measurements. In: Selected topics in radiation dosimetry. International Atomic Energy Agency, 1961. p. 161-172.

57. Lin, F. M. and J. R. Cameron. A bibliography of thermoluminescent dosimetry. Health Physics 14:495-514. 1968.

58. Loevinger, R. and S. S. Yaniv. Absorbed dose determination for x-rays in the grenz-ray region (5 to 20 keV quantum energy). Physics in Medicine and Biology 10:213-227. 1965.

59. Magnuson, C. E. Alternating currents. 5th ed. New York, McGraw-Hill Book Co., 1939. 721 p.

60. Marrone, M. J. and F. H. Attix. Damage effects in Ca_2F:Mn and LiF thermoluminescent dosimeters. Health Physics 10:431-436. 1964.

61. Mayneord, W. V. and L. F. Lamerton. A survey of depth dose data. British Journal of Radiology 14:255-264. 1941.

62. McCall, R. C., L. E. Babcock and R. C. Fix. LiF thermoluminescent dosimeter system for radiation research. Radiation Research 19:200. 1964.

63. McGinnies, R. T. X-ray attenuation coefficients from 10 keV to 100 MeV. Washington, D. C. 1959. 10 p. (U. S. National Bureau of Standards supplement to circular 583.)

64. Meiler, J. Drehstromgenerator und roentgenaufnahmetechnik. Acta Radiologica Therapy Physics Biology 4:401-414. 1966.

65. Meredith, W. J. and J. B. Massey. Fundamental physics of radiology. Baltimore, Williams and Wilkins, 1968. 599 p.

66. Meredith, W. J. and G. J. Neary. The production of isodose curves and the calculation of energy absorption from standard depth dose data. British Journal of Radiology 17:75-82. 1944.

67. Morgan, J. A. The development and application of multiphase x rays in medical radiography. Radiologic Technology 40:57-67. 1968.

68. National Council on Radiation Protection and Measurements. Medical x-ray and gamma-ray protection for energies up to 10 MeV. Washington, D. C., 1968. 66 p.

69. Naylor, G. P. The application of thermoluminescent phosphors in dosimetry problems in radiotherapy and radiobiology. British Journal of Radiology 40:170-176. 1967.

70. North American Philips, Inc. Three-phase vs. single-phase generators. New York, March 25, 1964. 4 p.

71. Oliver, R. and L. A. W. Kemp. An investigation into some factors affecting x-ray dose distribution and its measurements. British Journal of Radiology 22:33-43. 1949.

72. Palmer, R. C. A prototype LiF radiation dosimeter for personnel monitoring. International Journal of Applied Radiation and Isotopes. 17:413-416. 1966.

73. Parker, H. M. Dosage measurements by simple computations. Radiology 32:591-597. 1939.

74. Picker X-Ray Corporation. The production of x rays, a matter of energy conversion. White Plains, N. Y., n. d. 12 p.

75. Picker X-Ray Corporation. Three-phase generation of x rays. White Plains, N. Y., n. d. 4 p.

76. Quimby, E. H. The measurement of tissue dose in radiation therapy. Radiology 32:583-590. 1939.

77. Quimby, E. H. and R. F. McNattin. The change in quality of roentgen rays on passing through tissue. American Journal of Roentgenology and Radium Therapy 28:236-244. 1932.

78. Ridgway, A. and W. Thumm. The physics of medical radiography. Reading, Mass., Adison-Wesley, 1968. 494 p.

79. Ryder, J. D. Engineering electronics. New York, McGraw-Hill, 1957. 666 p.

80. Sanford, F. Electric distribution fundamentals. New York, McGraw-Hill Book Company, 1940. 242 p.

81. Schulman, J. H. et al. New thermoluminescent dosimeter. Review of Scientific Instruments 31:1263-1269. 1960.

82. Schulman, J. H. et al. Thermoluminescent dosimeter has storage stability, linearity. Nucleonics 18(3):92-102. 1960.

83. Seelye, H. P. Electrical distribution engineering. New York, McGraw-Hill Book Company, 1930. 710 p.

84. Shambon, A. and J. E. McLaughlin. Low dose measurements with thermoluminescent dosimeters. Health Physics 15:177. 1968.

85. Skarsgard, L. D. and H. E. Johns. Spectral flux density of scattered and primary radiation generated at 250 kV. Radiation Research 14:231-260. 1961.

86. Spiers, F. W. Effective atomic number and energy absorption in tissues. British Journal of Radiology 19:52-63. 1946.

87. Spiers, F. W. Materials for depth dose phantoms. British Journal of Radiology 16:90-97. 1943.

88. Spurny, Z. Additional bibliography of thermoluminescent dosimetry. Health Physics 17:349-354. 1969.

89. Suntharalingam, N. and J. R. Cameron. Absence of fading in LiF (TLD-100). Physics in Medicine and Biology 11:624. 1966.

90. Suntharalingam, N. et al. Fading characteristics of thermoluminescent lithium fluoride. Physics in Medicine and Biology 13: 97-104. 1968.

91. Svarcer, V., J. F. Fowler and T. J. Deeley. Exit dose for lung fields measured by lithium fluoride. British Journal of Radiology 38:785-790. 1965.

92. Ter-pogossian, M. M. The physical aspects of diagnostic radiology. New York, Harper and Row, 1967. 426 p.

93. Tochilin, E. and N. Goldstein. Spectral measurements from pulsed x-ray generators. Health Physics 12:1705-1713. 1966.

94. Trout, E. D. The life history of an x-ray beam. Radiologic Technology 35:161-170. 1963.

95. Trout, E. D. Professor of Radiological Physics, Oregon State University, Dept. of General Science. Personal Communication. Corvallis, Oregon. April 10, 1970.

96. Trout, E. D. and J. P. Kelley. Instruments for dose measurement. In: The reduction of patient dose by diagnostic radiologic instrumentation, ed. by R. D. Moseley and J. A. Rust, Springfield, Ill., Charles C. Thomas, 1964. p. 34-52.

97. Trout, E. D. and J. P. Kelley. Scattered radiation in a phantom from diagnostic quality radiation. Radiology 85:546-554. 1965.

98. Trout, E. D., J. P. Kelley and A. C. Lucas. Determination of half-value-layers. American Journal of Roentgenology, Radium Therapy and Nuclear Medicine 84:729-740. 1960.

99. Trout, E. D., J. P. Kelley and A. C. Lucas. Influence of cable length on dose rate and half-value-layer in diagnostic x-ray procedures. Radiology 74:255-264. 1960.

100. Wagner, J. and J. R. Cameron. The effect of the quality of radiation on the thermoluminescence of LiF (TLD-100). Wisconsin University, Madison. Dept. of Physics, July 15, 1966. (Progress Report, AEC Contract AT(11-1)-1105. 8 p.)

101. Wallace, D. M. and L. L. Watkins. Radiation response of LiF at low doses. Health Physics 15:159-160. 1968.

102. Watson, J. C., A. S. Weinstein and R. H. Greenspan. Advantages of three-phase spot film radiography. Radiology 79:973-978. 1962.

103. Weyl, C., S. R. Warren Jr., and D. B. O'Neill. Radiological physics. Springfield, Ill., Charles C. Thomas, 1941. 459 p.

104. Whyte, G. N. Principles of radiation dosimetry. New York, John Wiley and Sons, 1959. 124 p.

105. Worton, R. G. and A. F. Holloway. Lithium fluoride thermoluminescence dosimetry. Radiology 87:938-943. 1966.

106. Young, M. E. J. Radiological physics. 2d. ed. Springfield, Ill, Charles C. Thomas, 1967. 601 p.

107. Zimmerman, D. W., C. R. Rhyner and J. R. Cameron. Thermal annealing effects on the thermoluminescence of LiF. Health Physics 12:525-531. 1966.

APPENDIX

APPENDIX

X-RAY EQUIPMENT MANUFACTURERS PRESENTLY MARKETING THREE-PHASE APPARATUS

Balteau Co.	Liege, Belgium
Chenaille Corp.	Saint-Cloud, France
Chirana Naradni Podnik Co.	Prague, Czechoslovakia
Compagnie Generale de Radiologie	Issy-les-Moulineaux, France
Elema-Schonander Co.	Solna, Sweden
General Electric Co.	Milwaukee, Wis., U. S. A.
Gilardoni Co.	Mandello Lario, Italy
Keleket/CGR	Waltham, Mass., U. S. A.
Koch and Sterzel	Berlin, West Germany
North American Philips, Inc.	New York, N. Y., U. S. A.
Picker X-Ray Corp.	Cleveland, O., U. S. A.
Profexray	Des Plaines, Ill., U. S. A.
Rangoni and Puricelle	Bologna, Italy
Siemens Corp.	Erlangen, West Germany
Sierex Ltd.	London, England
Transformatoren und Rontgenwerk	Dresden, East Germany
Watson and Sons	Wembley, England
Westinghouse Corp.	Baltimore, Md., U. S. A.

CALCULATION OF PEAK, AVERAGE, AND ROOT-MEAN-SQUARE VOLTAGE AND CURRENT FOR SINGLE- AND THREE-PHASE X-RAY GENERATORS

These calculations are for generators operating at a peak voltage of 100 kilovolts and an average current of 100 milliamperes and assume sinusoidal waveforms.

The average and root-mean-square (rms) values of the positive cycle of a sine wave are 0.637 and 0.707 times the peak value, respectively (79).

For single-phase:

Average voltage = .637 x 100 kV = 63.7 kV

Rms voltage = .707 x 100 kV = 70.7 kV

Peak current = 100/.637 = 157 mA

Rms current = .707 x 157 = 111 mA

Three-phase waveforms may be considered to be composed of a constant component with a ripple superimposed. The voltage ripples for 6-pulse and 12-pulse generators are 13.5 kV and 3.4 kV, respectively. The corresponding constant components are 86.5 kV and 96.6 kV, respectively.

The average and rms three-phase voltages are equal to the constant components plus the respective average and rms components.

Average 6-pulse kilovoltage = 86.5 + .637 x 13.5 = 95.1 kV

Average 12-pulse kilovoltage = 96.6 + .637 x 3.4 = 98.8 kV

Rms 6-pulse kilovoltage = 86.5 + .707 x 13.5 = 96.0 kV

Rms 12-pulse kilovoltage = 96.6 + .707 x 3.4 = 99.0 kV

The current ripples for 6-pulse and 12-pulse generators are .135 and .034 times the peak current, respectively. The corresponding constant components are .865 and .966 times the peak current, respectively.

The average three-phase current is equal to the constant component plus the average of the ripple.

For 6-pulse generators:

100 = .865 x peak + .637 x .135 x peak

peak current = 105 mA

For 12-pulse generators:

100 = .966 x peak + .637 x .034 x peak

peak current = 101 mA

The rms three-phase current is equal to the constant component plus the rms of the ripple.

For 6-pulse generators:

rms current = .865 x 105 + .707 x .135 x 105

= 105 mA

For 12-pulse generators:

rms current = .966 x 101 + .707 x .034 x 101

= 100 mA